1959

Frequency response of rotating servo components

Yehuda Rachovitsky

Department:

FREQUENCY RESPONSE OF ROTATING SERVO COMPONENTS

BY

YEHUDA RACHOVITSKY

A

THESIS

submitted to the faculty of the

SCHOOL OF MINES AND METALLURGY OF THE UNIVERSITY OF MISSOURI

in partial fulfillment of the work required for the

Degree of

MASTER OF SCIENCE IN ELECTRICAL ENGINEERING

Rolla, Missouri

1959

Approved by

R. E. Wood (advisor) S. J. Pagano

Roger E. Wolfe J. J. Biagi

ACKNOWLEDGEMENT

The author of this thesis wishes to express his appreciation to Professor Israel H. Lovett, Chairman of the Electrical Engineering Department for his assistance in providing the author with graduate assistantship, and to others who have provided the equipment, with which the work has been made possible.

The author is greatly indebted to Mr. Robert T. DeWoody, Professor in Electrical Engineering, for his valuable advice and consultation during the course of this investigation.

TABLE OF CONTENTS

Acknowledgment ii

List of Tables v

List of Illustrations vi

Introduction 1

Chapter

1. Analytical Determination of Frequency Response . 3

D-c System 3

General Relationship for Separately Excited Shunt Motor 3

The Motor Transfer Function 5

The Motor Moment of Inertia 7

The Motor Constants 13

Open Loop Characteristics of Amplidyne and Motor 17

A-c System 25

Operating Characteristics of 2-Phase Induction Motor 25

System Damping Factor 27

The Motor-Load Transfer Function 31

2. Graphicl Determination of Frequency Response . . 33

D-c System 34

Description of System Tested 34

Principle of Operation 34

Frequency Response from Experimental Data . . 39

A-c System 53
Description of System Tested 53
Principle of Operation 53
Frequency Response from Experimental Data . . 55
3. Summary and Conclusion 69
Summary 69
Conclusion 72
Bibliography 73
Vita 74

LIST OF TABLES

TABLE		PAGE
I.	No-load Test of the D-c Motor	10
II.	Calculated a and J from Figure 3	12
III.	Load Test of the D-c Motor	14
IV.	No-load Test of the Amplidyne	23
V.	D-c System Frequency Response Experimental Data	42
VI.	D-c System Frequency Response Theoretical Data	44
VII.	Phase Shift Variation of Determined Transfer Function	46
VIII.	A-c System Frequency Response Experimental Data	56
IX.	The Amplifier Frequency Response	57

LIST OF ILLUSTRATION

FIGURE		PAGE
1.	Schematic Diagram of a D-c Motor	4
2.	Magnetization Curve	4
3.	Recorded Retardation Curve	8
4.	Retardation Curve - Larger Scale	9
5.	No-load Characteristic of the D-c Motor	11
6.	Speed-Torque Characteristics of the D-c Motor	15
7.	The Motor Torque as a Function of Armature Current	16
8.	Amplidyne - Motor Control System	18
9.	The Amplidyne Schematic Diagram	20
10.	The Amplidyne No-load Characteristics	24
11.	Speed-Torque Characteristics of the A-c Motor	26
12.	A-c System Gear Train	28
13.	Tachometer Response for Determining the A-c System Friction	30
14.	Schematic Diagram of D-c System Tested	35
15.	Block Diagram of the D-c System	36
16.	Schematic Setup for Measuring the D-c System Frequency Response	37
17.	D-c System - Schematic Diagram of the Electronic Amplifier	38
18.	D-c System - The Recorded Input and Output Signals	40

19. D-c System Frequency Response 47
20. D-c System Gear Train 48
21. D-c System - Control Transformer Characteristics 49
22. Polar Plot of D-c System Frequency Response . . . 50
23. High Frequency Portion of the Polar Plot of the D-c System 51
24. Comparison of Analytically and Experimentally Obtained D-c System Frequency Response 52
25. Schematic Diagram of A-c System Tested 58
26. Block Diagram of the System 59
27. Schematic Setup for Measuring the A-c System Frequency Response 60
28. A-c System - Schematic Diagram of the
(a) Voltage Amplifier 61
(b) Power Amplifier 62
29. A-c System - The Recorded Input and Output Signals 63
30. Scope Patterns for Determining Phase shift in A-c System 64
31. A-c System - Gain Variation with Frequency . . 65
32. A-c System - Phase Variation with Frequency . . 66
33. Determination of A-c Motor Frequency Response . . 67
34. Comparison of Analytically and Experimentally Obtained A-c System Frequency Response 68

INTRODUCTION

The frequency response approach to the design of automatic controls is the dominant one today. This approach in a strict sense may be said to have started with a paper in 1932 by Dr. H. Nyquist, a physicist at the Bell Telephone Laboratories. In this paper Dr. Nyquist was concerned with the stability of feedback amplifiers. This work can be said to have made possible the transcontinental telephone as well as modern radio and television. Dr. Hendrick Bode, mathematician at the Bell Laboratory, extended the results of Dr. Nyquist and obtained some simple design criteria that enabled even technicians without much mathematical training, to determine whether or not a system is stable.

In the study of physical devices one is generally concerned with inputs and outputs to the devices. As the inputs are varied the outputs are affected. This study is often reduced to that of the relation between one input and one output.

In a broad sense the frequency response approach to the design of a physical device, may be said to be that in which use is made of the response of the output of the device to sinusoidal oscillation of the input.

The needed information about the system is visualized easier from the frequency response curves, than from the differential equations. In writing down the differential

equations for a physical system the dominant factors need to be considered. Except for errors in measurement, the experimental frequency response curves for a physical device truly represent this device.

The system frequency response is much affected by the behaviour of its components with variation of the frequency. The frequency response of each component should be on hand before the overall frequency response has to be predicted theoretically. Experimental frequency response will give more accurate results, because a simple analytical approach does not involve the nonlinear effects of the components characteristics.

CHAPTER 1

ANALYTICAL DETERMINATION OF FREQUENCY RESPONSE

D-C SYSTEM

General Relationship for Separately Excited Shunt Motor

For a d-c machine as shown in Figure 1, the following relationships exist:

Armature circuit: $$V_m = E_g + I_m R_m + L_m \frac{dI_m}{dt} \quad (1)$$

Field circuit: $$V_f = I_f R_f + L_f \frac{dI_f}{dt} \quad .... \quad (2)$$

Electromechanical coupling: $$E_g = K_e w \quad ..... \quad (3)$$

$$T = K_t I_m \quad ..... \quad (4)$$

where V_m - armature voltage, volts

I_m - armature current, amperes

R_m - armature resistance, Ohms

L_m - armature inductance, Henries

E_g - back emf, volts

I_f - field current, amperes

R_f - field resistance, Ohms

L_f - field inductance, Henries

w - angular velocity, sec^{-1}

K_t - torque constant, in-oz/amp.

K_e - back emf constant, volt-sec.

T - developed torque, in-oz.

The accuracy of the above equations is limited by nonlinearities in the various circuits. For example, the brushes in the armature circuit obey Ohm's law only at low load. But as the brush resistance is small compared to the overall armature

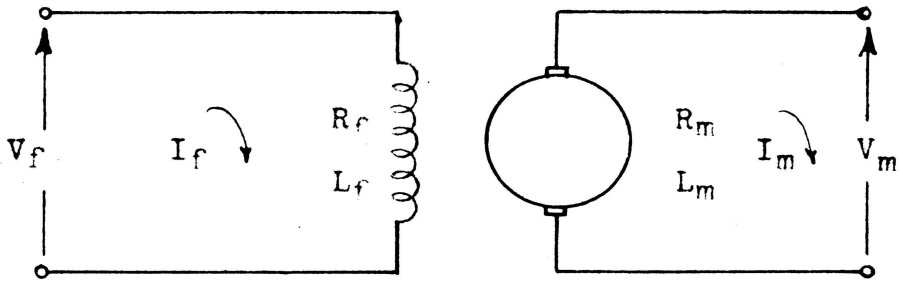

FIGURE 1

SCHEMATIC DIAGRAM OF A D-C MOTOR

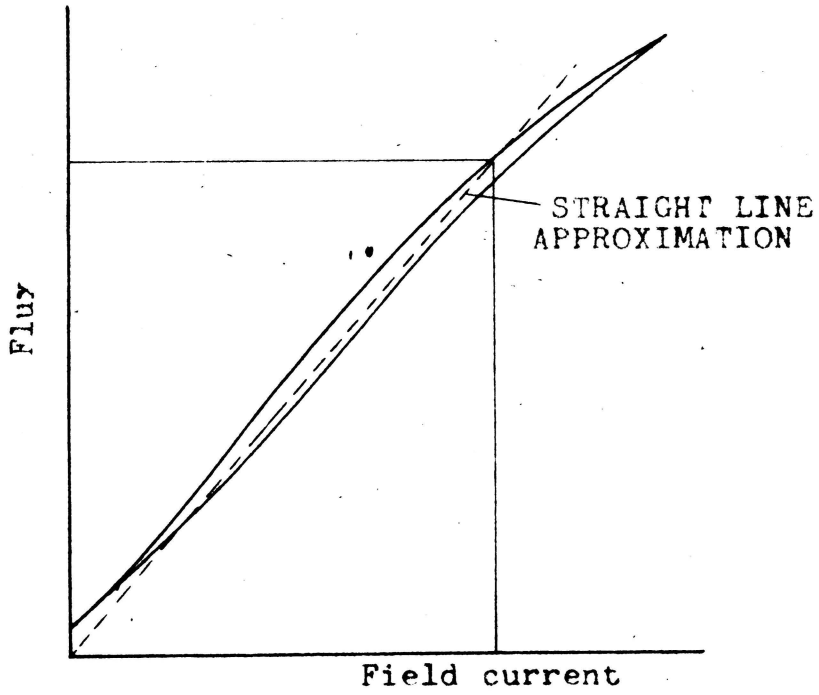

FIGURE 2

MAGNETIZATION CURVE

resistance this nonlinearity can be neglected. The main cause for nonlinearity in the motor is the relationship between the air-gap flux and the field current, which can be shown by the magnetization curve in Figure 2. If the operation of the motor is kept below the knee of the magnetization curve, approximation of a straight line can be made. If a strong field that saturates the magnetic circuit is applied, these nonlinearities have no influence. Actually, the field of highly-saturated d-c machine remains quite constant.

The effect of armature reaction in reducing the main field is cancelled as much as possible by means of compensating fields. On the other hand, if the motor is controlled by varying the field current, non-linear operation of the motor is expected. A good example for this is the series motor (which will not be discussed here).

The Motor Transfer Function [1,2,3]

Assuming that the flux remains constant and substituting equations (3) and (4) in (1),

$$V_m = K_e w + \frac{R_m}{K_t} T + \frac{L_m}{K_t} \frac{dT}{dt} \quad \ldots\ldots\ldots\ldots\ldots (5)$$

With the conditions of constant applied voltage and zero rate of change of torque, corresponding to steady state condition of the speed-torque characteristics, we obtain equation (6)

$$T = (V_m - K_e w)\frac{K_t}{R_m} \quad \ldots\ldots\ldots\ldots\ldots\ldots (6)$$

Equation (6) is a family of straight lines whose constants may be found from the torque -speed characteristics:

1. All references are in bibliography.

$$\frac{K_t}{R_m} = \frac{\partial T}{\partial V_m} \quad \text{..... (7)}$$

$$-\frac{K_e K_t}{R_m} = \frac{\partial T}{\partial w}$$

Using eq. (7) $$T = \frac{\partial T}{\partial V_m} V_m + \frac{\partial T}{\partial w} w \quad \text{..... (8)}$$

If the mechanical load on the motor consists of inertia J and viscous friction f, then we have

$$T = J \frac{dw}{dt} + fw \quad \text{..... (9)}$$

using eq. (8) and substitute eq. (7) we have

$$T = V_m \frac{K_t}{R_m} - \frac{K_e K_t}{R_m} w \quad \text{..... (10)}$$

By the method of Laplace transformation and remembering that

$$w = \frac{d\theta}{dt} = p\theta \quad \text{.....(11)}$$

then obtain

$$\theta = \frac{V_m\left(\frac{K_t}{R_m}\right)}{p\left(Jp + f + \frac{K_e K_t}{R_m}\right)} \quad \text{.....(12)}$$

where J and f are the combined motor and load moment of inertia and friction. Or in the usual form:

$$\frac{\theta}{V_m} = \frac{K_m}{p(T_m p + 1)} \quad \text{..... (13)}$$

where

$$K_m = \frac{K_t}{R_m\left(f + \frac{K_e K_t}{R_m}\right)}$$

$$T_m = \frac{J}{f + \frac{K_e K_t}{R_m}}$$

The Motor Moment of Inertia[4]

The retardation method was used to find the motor moment of inertia. The Kinetic energy of the rotor is equal to

$$W = \tfrac{1}{2}w^2J \qquad \text{..... (14)}$$

where W, w, and J are the kinetic energy, the angular velocity and the moment of inertia of the motor.

Differentiating with respect to t

and the power $$P = \frac{dW}{dt} = Jw\frac{dw}{dt}$$

or $$P = Jwa \qquad \text{..... (15)}$$

The no-load loss at any speed is equal to the friction, windage, core and a small armature copper loss, at the same speed. Using those values of power, speed and retardation (evaluated from the retardation curve) the motor moment of inertia can be found. The motor speed-time characteristic, when retarded from 2000 rpm with closed field circuit was recorded directly by means of the Brush Recorder and a small tachometer. The recorded response is shown in Figure 3. A larger scale is used in Figure 4 in order to calculate the retardation values. The corresponding values of power were taken from the no-load characteristic of the motor given in Figure 5.

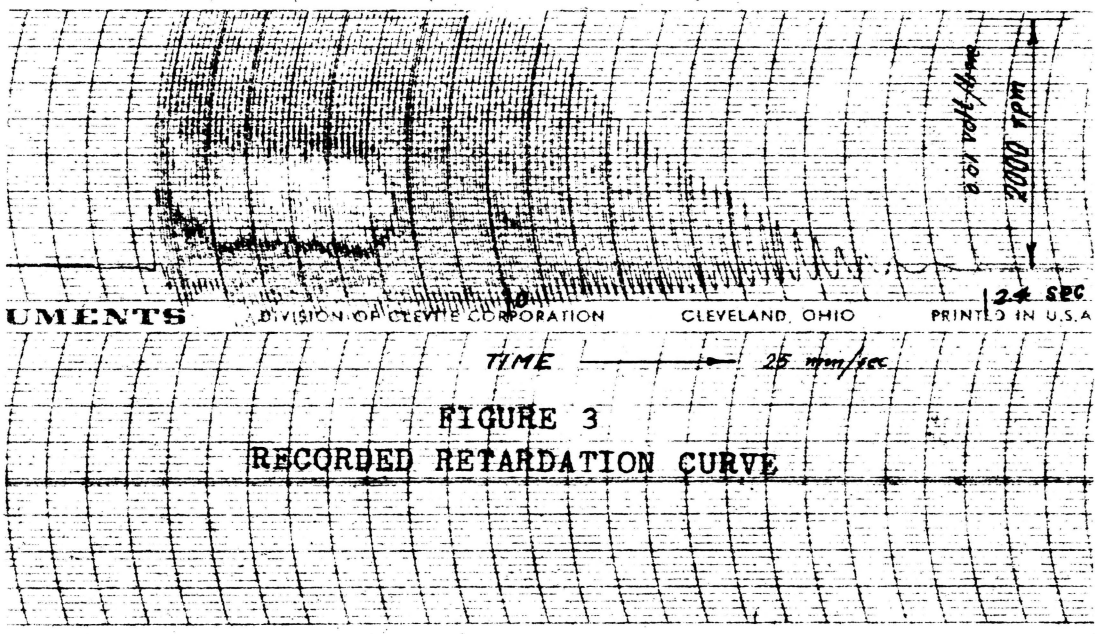

FIGURE 3
RECORDED RETARDATION CURVE

MOTOR INFORMATION:

220 volts
1/4 HP
1.3 amperes
1750 rpm

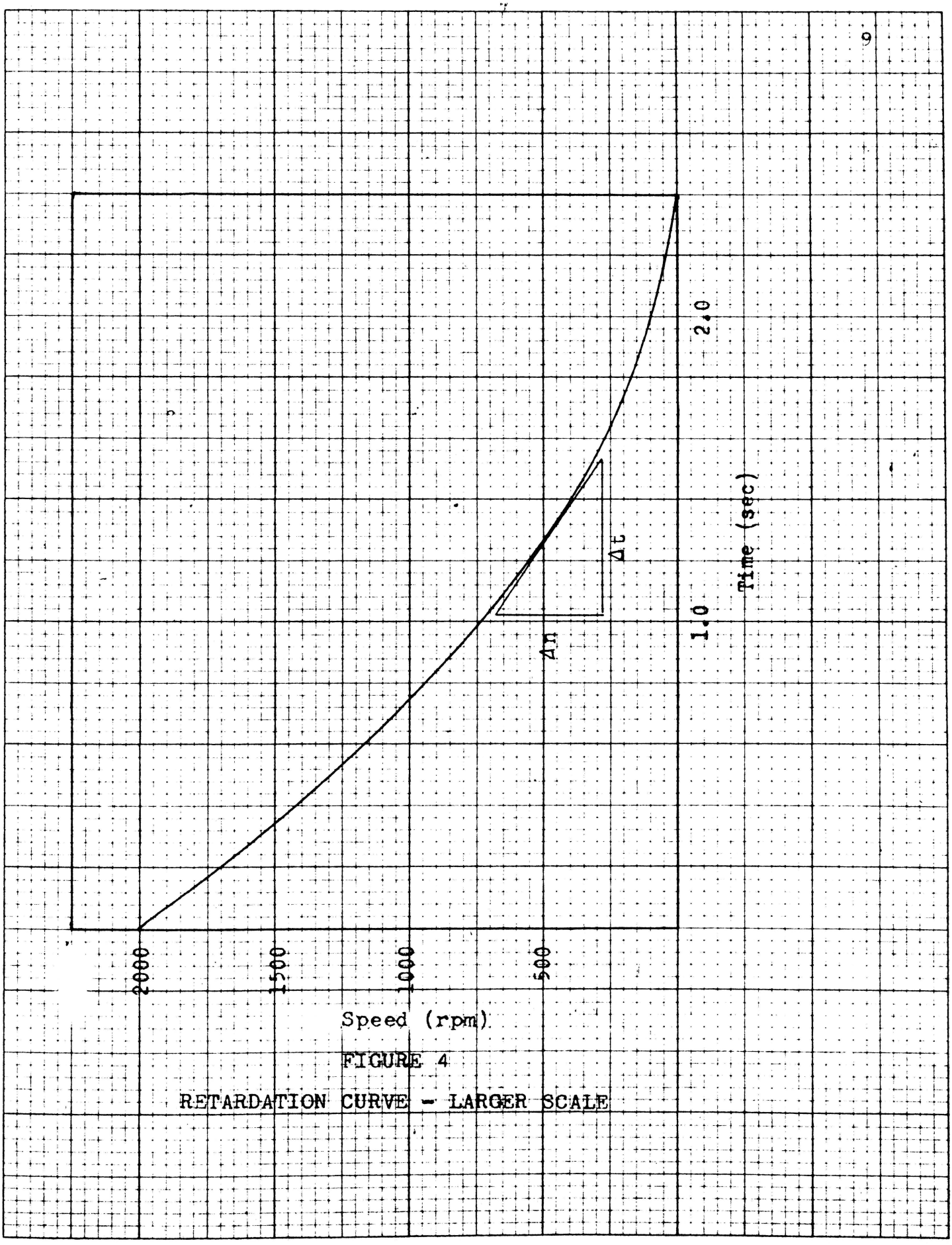

FIGURE 4

RETARDATION CURVE - LARGER SCALE

TABLE I

NO LOAD TEST OF THE D-C MOTOR

n rpm	I amps	V volts	P watts
600	0.100	60	6.0
800	0.107	86	9.2
1000	0.114	109	12.4
1200	0.118	132	15.6
1400	0.127	146	19.0
1600	0.141	170	24.0
1800	0.151	186	28.0

Using the values of power from Table I and the values of retardation evaluated from Figure 3, we obtain Table II, where

n - motor speed, rpm

w - motor speed, rad/sec

P - no load power input, watts

a - retardation, rad/sec^2

J - motor moment of inertia, in-oz. sec^2.

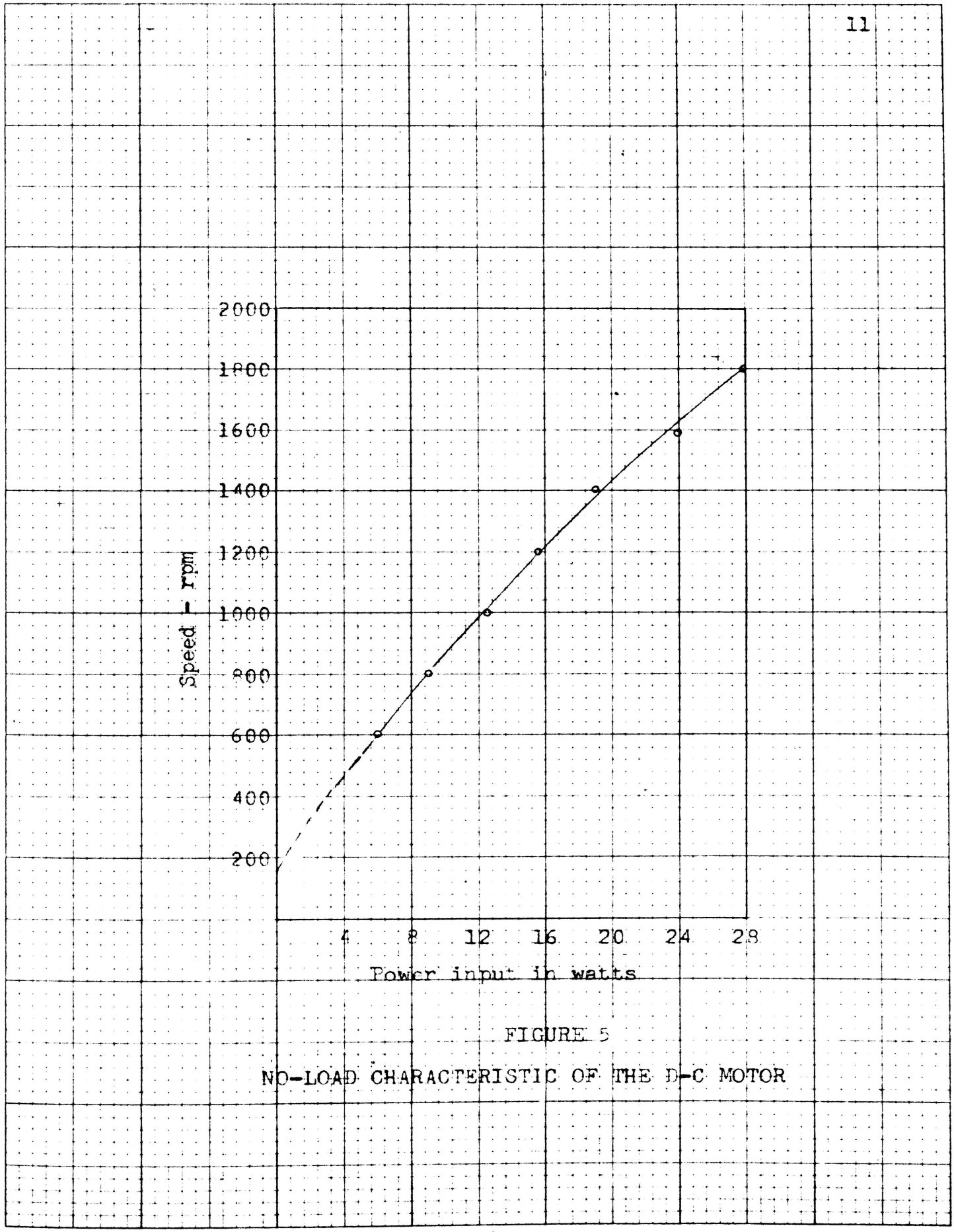

FIGURE 5

NO-LOAD CHARACTERISTIC OF THE D-C MOTOR

TABLE II

CALCULATED a AND J FROM FIGURE 3

n rpm	w sec^{-1}	a sec^{-2}	P watts	J in-oz.sec^2
600	62.8	89	6.0	0.152
800	83.5	107	9.2	0.143
1000	104.0	121	12.4	0.140
1200	125.0	130	15.6	0.136
1400	146.0	138	19.0	0.134
1600	167.0	147	24.0	0.139

Several values of inertia were calculated from which the value

$$J = 0.140 \text{ in-oz.sec}^2 \quad \ldots\ldots\ldots\ldots\ldots\ldots (16)$$

is the average value of the motor moment of inertia. The main sources of error in finding the moment of inertia is due to:

(1) Pressing a tachometer to the motor shaft causes another friction force.

(2) This force is not constant, (in 1).

(3) Nonlinearities in the tachometer characteristic.

The Motor Constants [5,6,7]

Using Figure 6 and equation (7), it can be shown that:

a) Damping constant.

$$\frac{\partial T}{\partial w} = \frac{K_e K_t}{R_m} \quad \frac{T_{stall}}{w_{no\text{-}load}} = 6.13 \text{ in-oz.sec}$$

b) The back emf constant.

$$\frac{\partial V_m}{\partial w} = K_e = 1.15 \text{ volts-sec.}$$

c) By plotting the torque as a function of the armature current the motor torque constant is obtained from Figure 7,

$$\tan\alpha = K_t = 123 \text{ in-oz/amp.}$$

and from Figure 6, it is easily confirmed that

$$K_t = \frac{\partial T}{\partial V_m} R_m = 5.33 \times 23 = 122.6 \text{ in-oz/amp.}$$

d) The motor gain.

Substitute the above values in equations (13) and neglect the motor viscous friction, then

$$K = \frac{K_t}{R_m(f + K_e K_t/R_m)} = \frac{1}{K_e} = 0.87 \text{ (volt.sec)}^{-1}$$

e) The motor time constant .

$$T_m = \frac{J}{f + K_e K_t/R_m} = 0.0228 \text{ sec}$$

Substituting the above values in equation (13) would result the motor transfer function:

$$\frac{\theta}{V_m} = \frac{0.87}{p(0.0288p + 1)} \quad \ldots\ldots\ldots\ldots \quad (17)$$

TABLE III

LOAD TEST OF THE D-C MOTOR

V volts	I amps	n rpm	T ft-lb
30	0.20	240	0.84
30	0.48	170	3.00
30	0.64	150	4.20
30	0.72	130	4.80
40	0.20	330	0.72
40	0.42	300	2.40
40	0.60	250	4.00
40	0.90	200	6.60
50	0.18	400	0.66
50	0.38	390	2.10
50	0.54	360	3.60
50	0.80	310	5.70
50	1.20	300	7.80
60	0.30	500	1.68
60	0.66	430	4.62
60	0.98	360	7.26
60	1.18	330	9.00
60	1.31	310	10.20
70	0.24	600	0.96
70	0.55	550	3.6
70	0.74	510	5.16
70	1.08	450	8.10
70	1.30	410	9.30
80	0.20	710	1.20
80	0.60	640	3.48
80	0.80	600	5.51
80	1.06	540	7.80
80	1.32	500	10.10
100	0.26	900	1.20
100	0.56	850	3.60
100	0.83	800	5.87
100	1.12	750	8.40
100	1.33	700	9.90

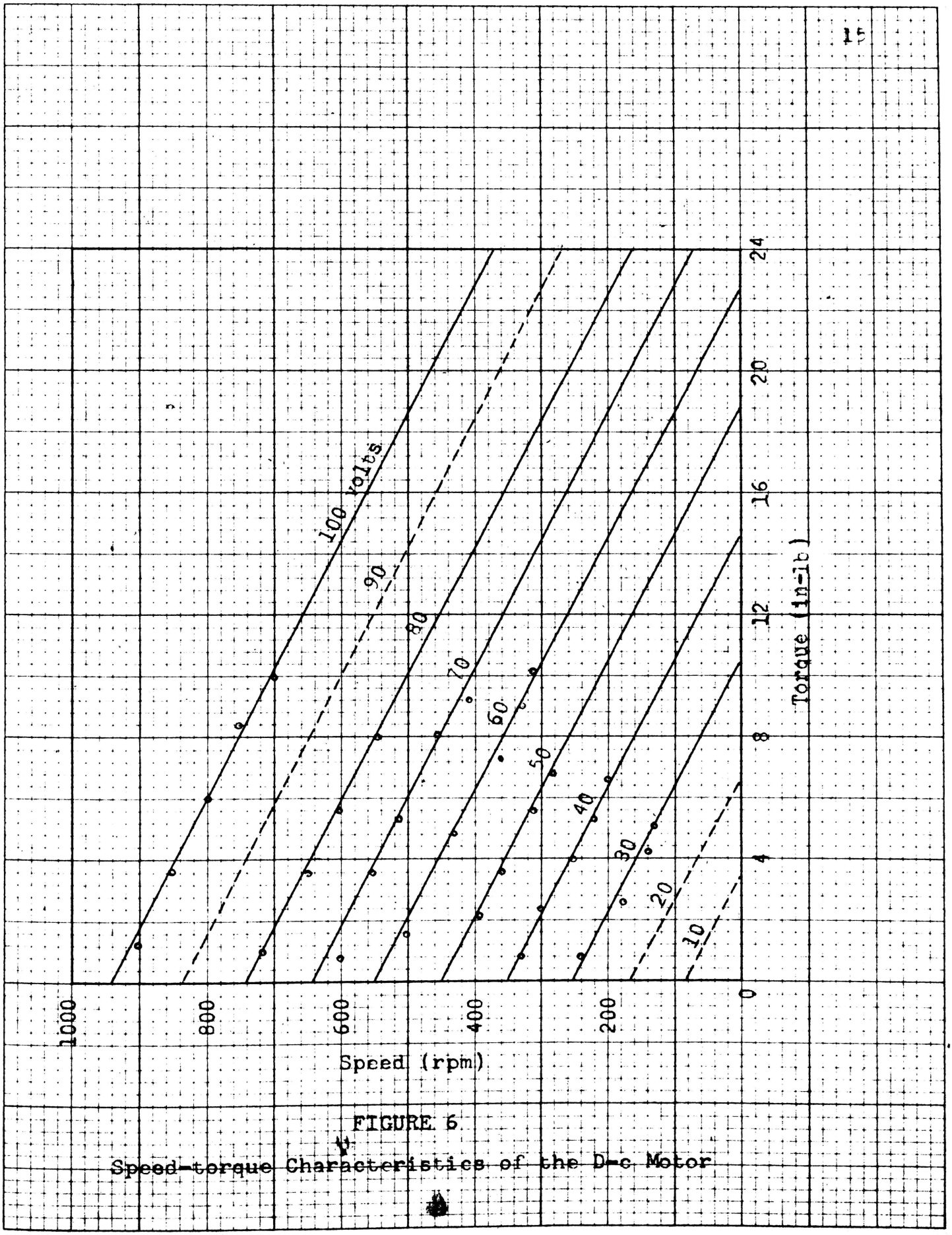

FIGURE 6

Speed-torque Characteristics of the D-c Motor

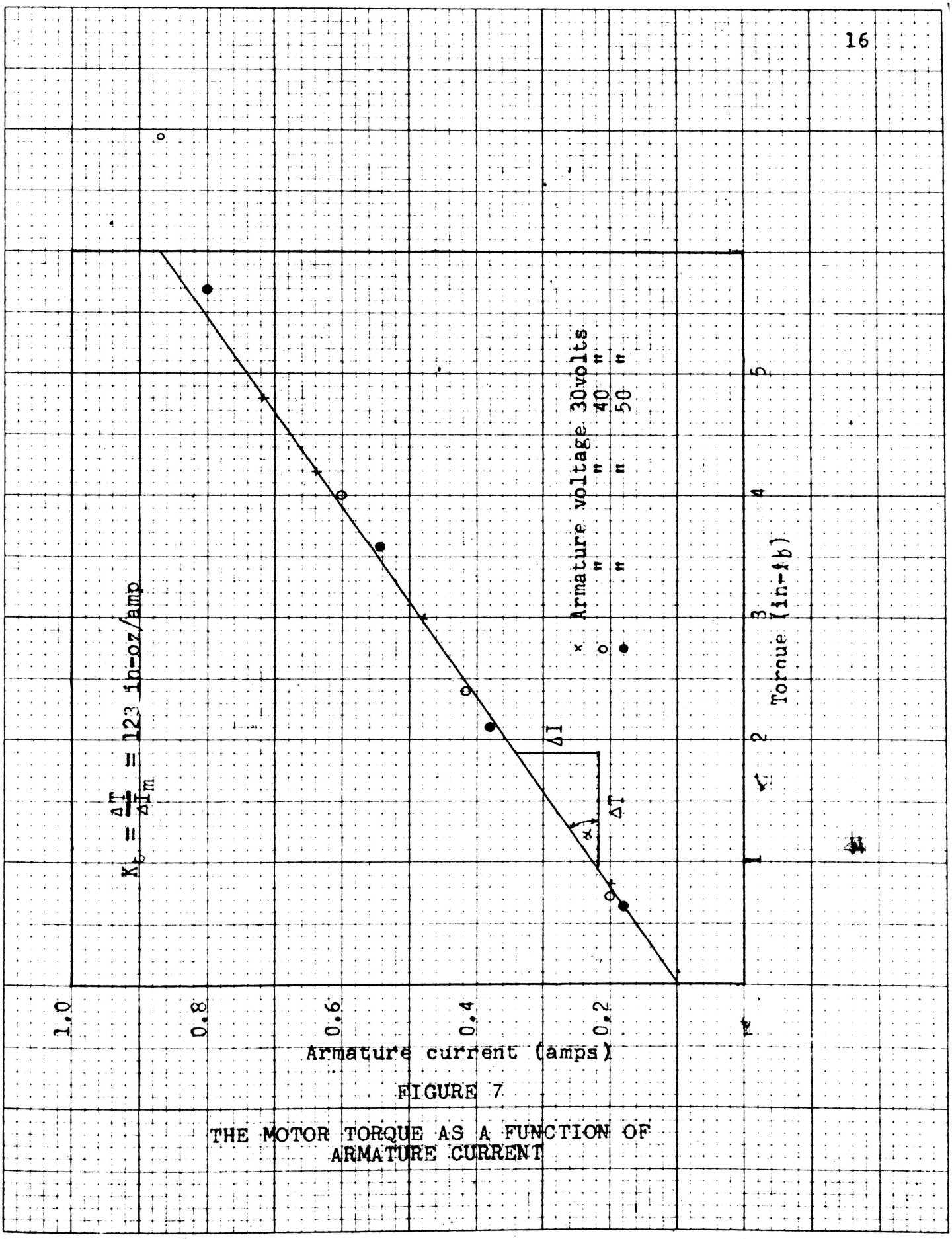

FIGURE 7

THE MOTOR TORQUE AS A FUNCTION OF ARMATURE CURRENT

Open-loop Characteristics of Amplidyne and Motor [7]

When an amplidyne is used to excite a d-c motor in a control system, (Figure 8), a transfer function can be found using the motor characteristics previously determined, but remembering that the motor armature circuit impedance is changed because a source of power having a certain amount of output impedance is applied.

a) The motor-load transfer function:

The voltage applied to the armature of the motor is the generated voltage of the amplidyne V_d.

$$V_d = I_m R(T_a p + 1) + K_e p\theta_m \quad \ldots\ldots\ldots\ldots (18)$$

where $R = R_d + R_m$

$$T_a = \frac{Ld + Lm}{R_d \quad R_m} \quad \ldots\ldots\ldots\ldots\ldots\ldots\ldots (19)$$

From equation (8)

$$I_m = \frac{V_d - K_e p\theta_m}{R(T_a p + 1)} \quad \ldots\ldots\ldots\ldots\ldots\ldots (20)$$

The torque results from the motor armature current I_m will be consumed in accelerating the inertia J_m of the motor, the inertia of the gear train J_g, and that of the load J_l, reduced to motor shaft; it also will be dissipated in overcoming any viscous friction in the fearing and bearing. Thus the torque equation is

$$Jp^2\ \theta_m + fp\theta_m = K_t I_m = K_t \frac{V_d - K_e p\theta_m}{R(T_a p + 1)} \quad \ldots\ldots\ldots (21)$$

Usually, and here,

$$\frac{J}{f} \gg T_a \ldots\ldots\ldots\ldots\ldots\ldots\ldots (22)$$

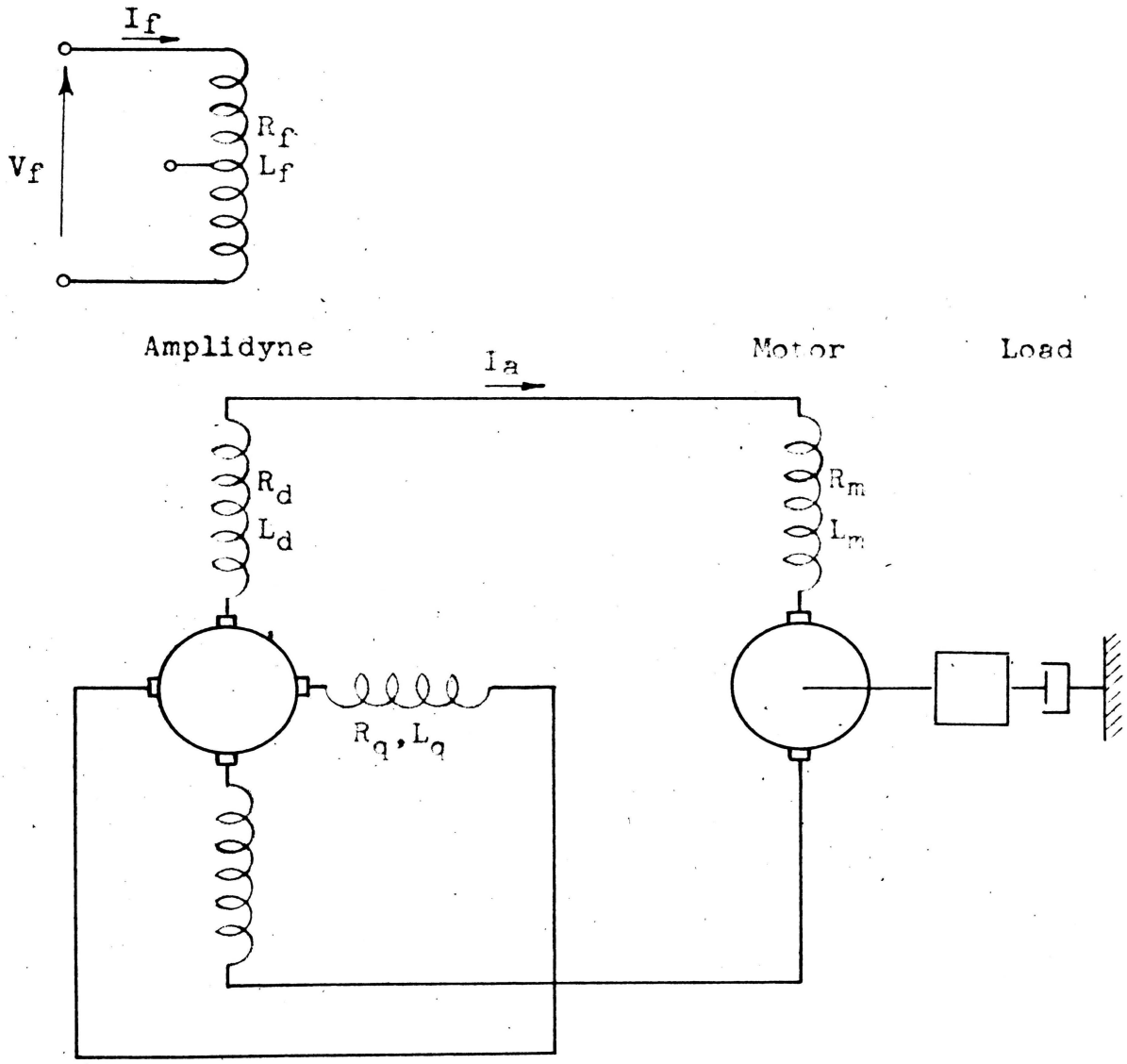

FIGURE 8

AMPLIDYNE - MOTOR CONTROL SYSTEM

and with this approximation

$$f\left(\frac{J}{f}p + 1\right)p\theta_m + \frac{K_tK_e}{R}p\theta_m = \frac{K_t}{R}V_d$$

$$\frac{K_t}{R}V_d = \left(Jp + f + \frac{K_tK_e}{R}\right)p\theta_m$$

or
$$\frac{K_t}{R}V_d = (T_{ma}\,p + 1)\left(f + \frac{K_tK_e}{R}\right)p\theta_m \quad \ldots\ldots\ldots\ldots (23)$$

where
$$T_{ma} = \frac{J}{f + \frac{K_tK_e}{R}} \quad \ldots\ldots\ldots\ldots\ldots\ldots\ldots\ldots (24)$$

and the motor-load transfer function will be

$$\frac{\theta_m}{V_d} = \frac{K_t/\,R(f + K_tK_e/R)}{p(T_{ma}p + 1)} \quad \ldots\ldots\ldots\ldots\ldots\ldots (25)$$

b) The amplidyne transfer function

The amplidyne constants as measured (see Figure 9) are:

Control field circuit: (F1-F4)	R_f =	1660 Ohms
	L_f =	90 Hy
Direct axis circuit: (C1-C4)	R_d =	56 Ohms
	L_d =	0.83 Hy
Quadrature axis circuit: (Armature circuit)	R_q =	26 Ohms
	L_q =	2 Hy

Data were taken for the no-load curve of the amplidyne when a full and a half field was excited (Table IV).

The control field circuit (Figure 8)

$$I_f = \frac{V_f}{R_f(T_fp + 1)} \quad \ldots\ldots\ldots\ldots\ldots (26)$$

The quadrature circuit

$$V_q = K_qI_f = \frac{K_qV_f}{R_q(T_qp + 1)} \quad \ldots\ldots\ldots\ldots\ldots (27)$$

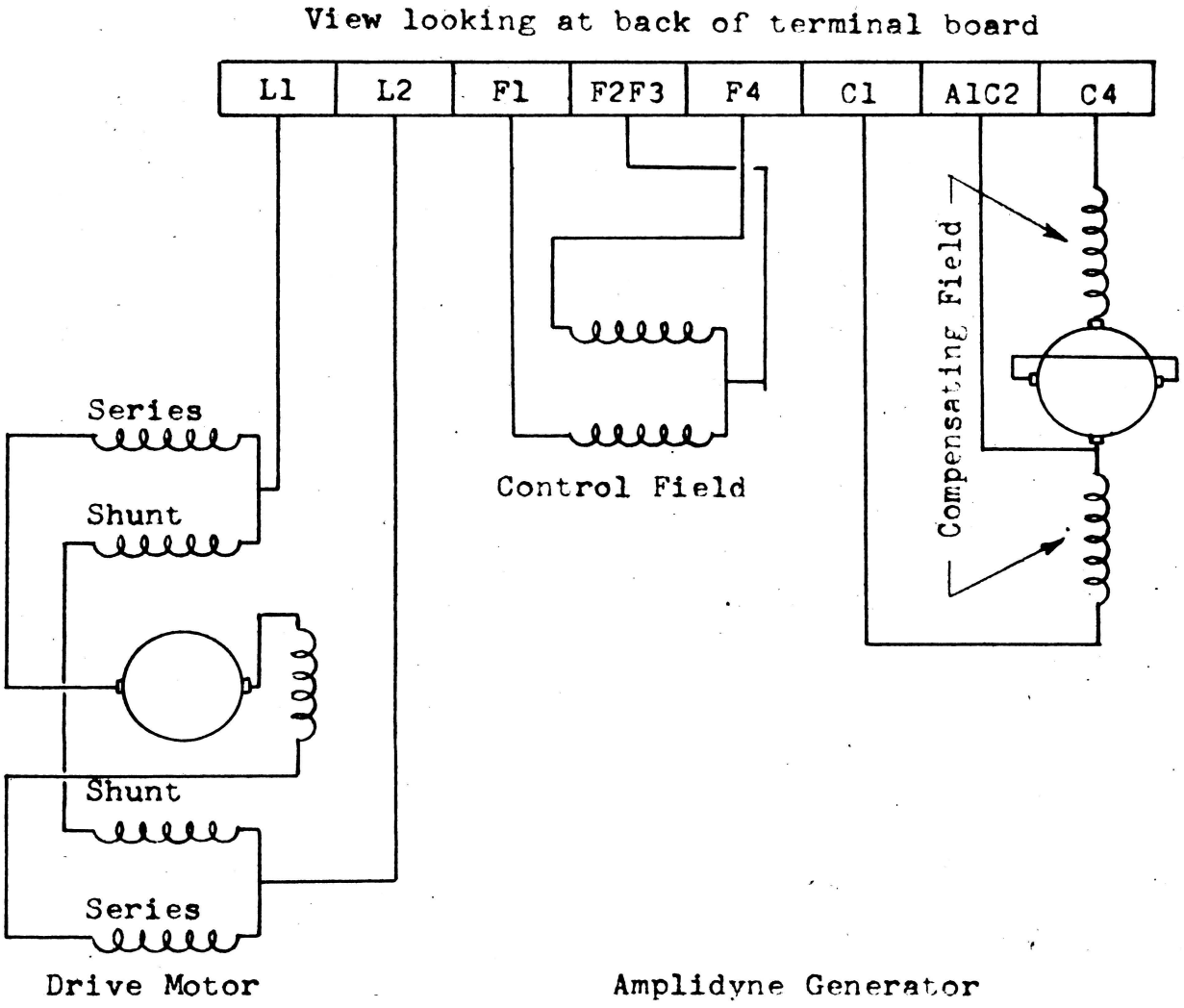

FIGURE 9

THE AMPLIDYNE SCHEMATIC DIAGRAM

Substituting equations (26) in (27)

$$I_q = \frac{K_q V_f}{R_f R_q (T_f p + 1)\ (T_q p + 1)} \quad \ldots\ldots\ldots\ldots\ldots\ldots \quad (28)$$

$$V_d = K_d I_q = \frac{K V_f}{R_f R_q (T_f p + 1)\ (T_q p + 1)} \quad \ldots\ldots\ldots\ldots \quad (29)$$

where $K = K_d K_q$

The unloaded amplidyne transfer function is therefore,

$$\frac{V_d}{V_f} = \frac{K/R_f R_q}{(T_f p + 1)\ (T_q p + 1)} \quad \ldots\ldots\ldots\ldots\ldots\ldots\ldots \quad (30)$$

When a current source is used to excite the amplidyne, the following expression will be found by substituting equation (26) in equation (30)

$$\frac{V_d}{I_f} = \frac{K/R_q}{T_q p + 1} \quad \ldots\ldots\ldots\ldots\ldots\ldots\ldots \quad (31)$$

From the no-load test, Figure 10, it is shown that for zero frequency

$$K_f = \frac{K}{R_q} = \left[\frac{V_d}{I_f}\right]_{w\,=\,o} = 41.5 \text{ volts/ma} \quad \ldots\ldots\ldots\ldots \quad (32)$$

substituting values in equation (31), then

$$\frac{V_d}{I_f} = \frac{41.5}{0.077p + 1} \quad \ldots\ldots\ldots\ldots\ldots\ldots\ldots \quad (33)$$

where $T_q = \frac{L_q}{R_q} = 0.077$ sec

knowing the constants and making use of

$k_t = 123$ in-oz/amp

$K_e = 1.15$ volt.sec

$$R = R_d + R_m = 56 + 23 = 79 \text{ Ohms}$$

$$J = 0.140 \text{ in-oz.sec}^2$$

it is found that by neglecting the motor friction,

$$\frac{K_t}{R(f + K_t K_e/R)} = \frac{1}{K_e} = 0.87 \text{ (volt.sec)}^{-1}$$

$$\frac{J}{f + K_t K_e/R} = \frac{0.140}{\frac{1.15 \times 123}{79}} = 0.078 \text{ sec}$$

and the motor-load transfer function would result

$$\frac{\Theta_m}{V_d} = \frac{0.87}{p(p.078p + 1)} \quad \ldots\ldots\ldots\ldots\ldots\ldots \quad (34)$$

The overall transfer function of the amplidyne-motor combination is

$$\frac{\Theta_m}{I_f} = \frac{\Theta_m}{V_d} \times \frac{V_d}{I_f} = \frac{36.1}{p(0.078p + 1)\ (0.077p + 1)} \quad \ldots\ldots\ldots\ldots \quad (35)$$

TABLE IV

NO LOAD TEST OF THE AMPLIDYNE

Full field		Half field	
I_f ma	V_d volts	I_f ma	V_d volts
0.0	5	0.0	8
1.0	33	1.0	20
1.3	40	1.6	34
1.6	50	2.3	48
1.8	60	3.3	70
2.3	76	4.1	87
2.6	88	5.0	104
3.0	102	5.5	120
3.3	113	5.9	130
3.7	130	6.6	149
4.1	146	7.4	167
4.4	160	8.0	181
4.8	176	8.5	194
5.2	194	9.0	206
5.6	210	9.7	223
6.5	245	10.5	244
6.7	260	11.3	258
7.0	278	12.2	280

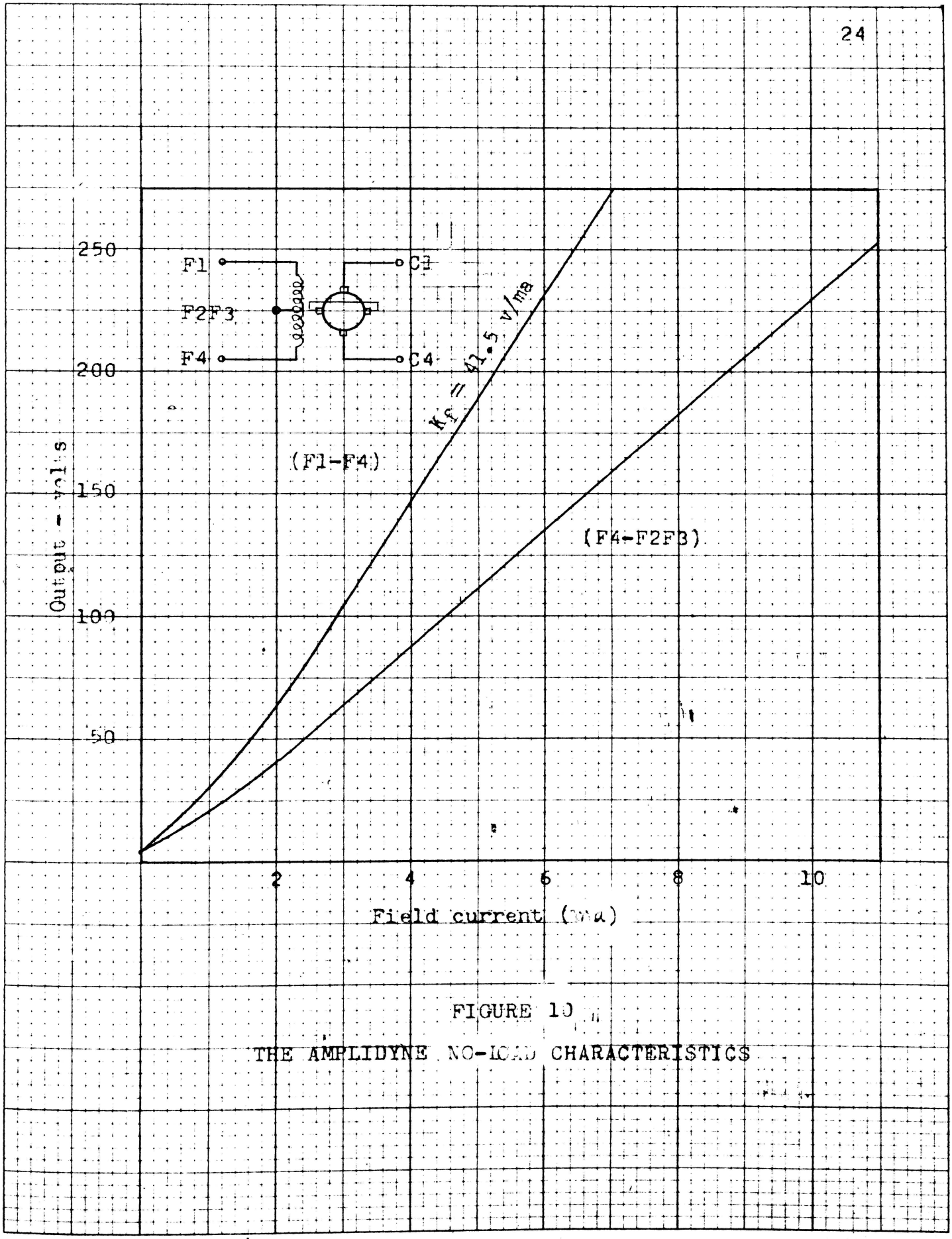

FIGURE 10

THE AMPLIDYNE NO-LOAD CHARACTERISTICS

A-C SYSTEM

Operating Characteristic of 2-phase Induction Motor

The operation of two-phase induction motor differs from that of conventional induction motor, principlly because the voltages applied do not constitute a balance polyphase set. The type of induction motors for servo work have very high rotor resistance and hence very low operating efficiencies. But on the other hand, the motor torque characteristic is fairly linear. Speed-torque curves for different values of control voltages were approximated from the characteristic given by M. A. Steinhacker and W. E. Meserve[8]. Those are given in Figure 11.

TABLE V

CHARACTERISTICS OF THE MOTOR (DIEL MFG.)

Style number	FP 25-2
Power output	2 watts
Poles	4
Frequency, cycles/sec.	60
Volts per phase	20
Amperes	0.85
Inertia, in-oz.sec^2 ..	0.508 x 10^{-3}

Discussion of Torque Coefficients

Since the motor is of 2-phase type, it is very sensitive to harmonics in the applied voltage wave. The expression of motor torque characteristic which can be

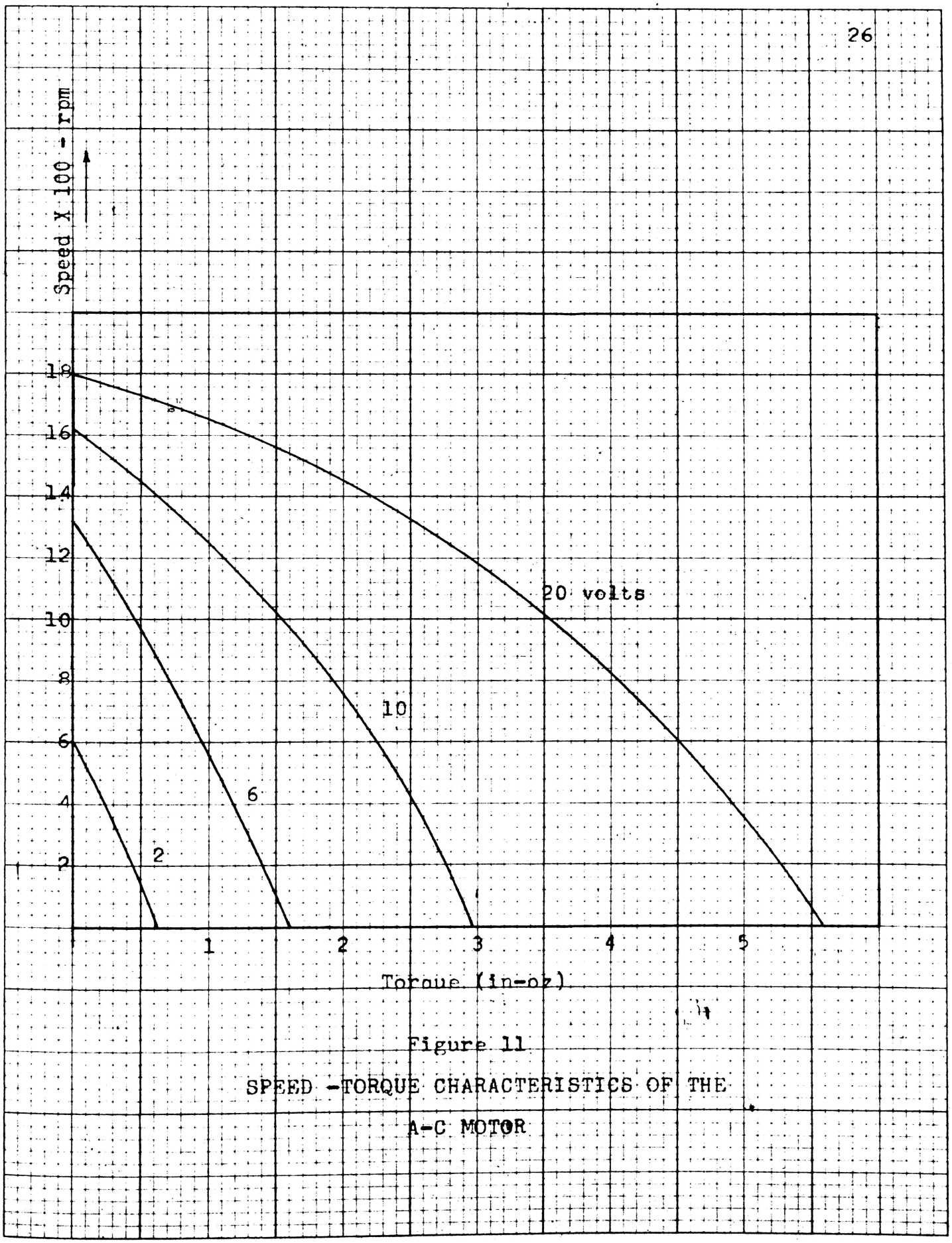

Figure 11

SPEED -TORQUE CHARACTERISTICS OF THE A-C MOTOR

used in servo system

$$T = \frac{\partial T}{\partial w} w + \frac{\partial T}{\partial V} V \quad \ldots\ldots\ldots\ldots\ldots\ldots\ldots\ldots \quad (36)$$

where w is the motor speed, and V is the control voltage. The use of the above equation involves determination of the coefficient $\partial T/\partial w$ in the neighborhood of the operating speed, and $\frac{\partial T}{\partial V}$ in the neighborhood of the operating control voltage. Observation of Figure 11 shows that for speeds below 1000 rpm the speed-torque curves are of fairly constant slope. Therefore, the assumption that $\partial T/\partial w$ is a constant value over the normal range encountered in zeroing operation gives fairly accurate results. Since during the zeroing period, the speed-torque curves are fairly parallel, and indication of the value $\partial T/\partial V$ can be obtained by using the blocked or zero speed values.

System Damping Factor

The system damping factor consists of the motor damping constant and the system friction. The system friction is determined by the following method:

A very light and small wheel (made of wood) was attached to the shaft of gear Z_4, as shown in Figure 12-a. A weight of 200 grams was suspended on a string wound on this wheel, shown in Figure 12-b. By letting the system be free of any external forces except F, the weight will move downward due to gravity. The system will come to a steady state condition when the torque produced by F will be equal to the torque due to the friction of the system,

(a)

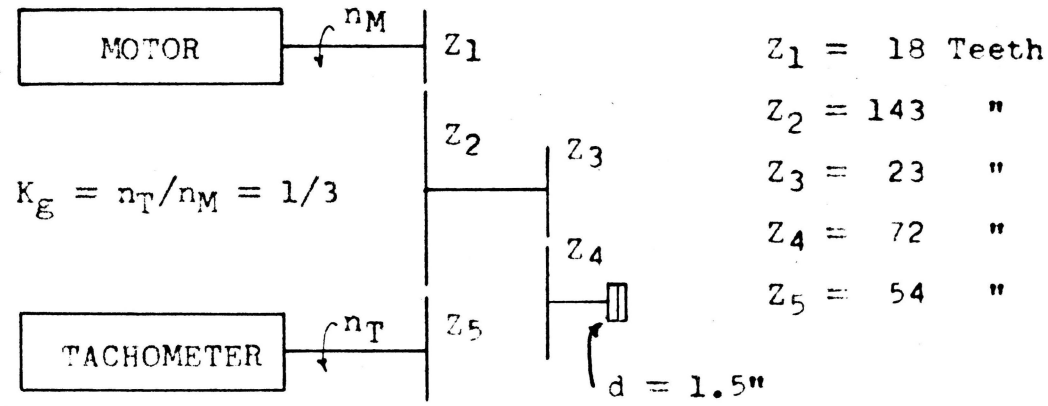

(b)

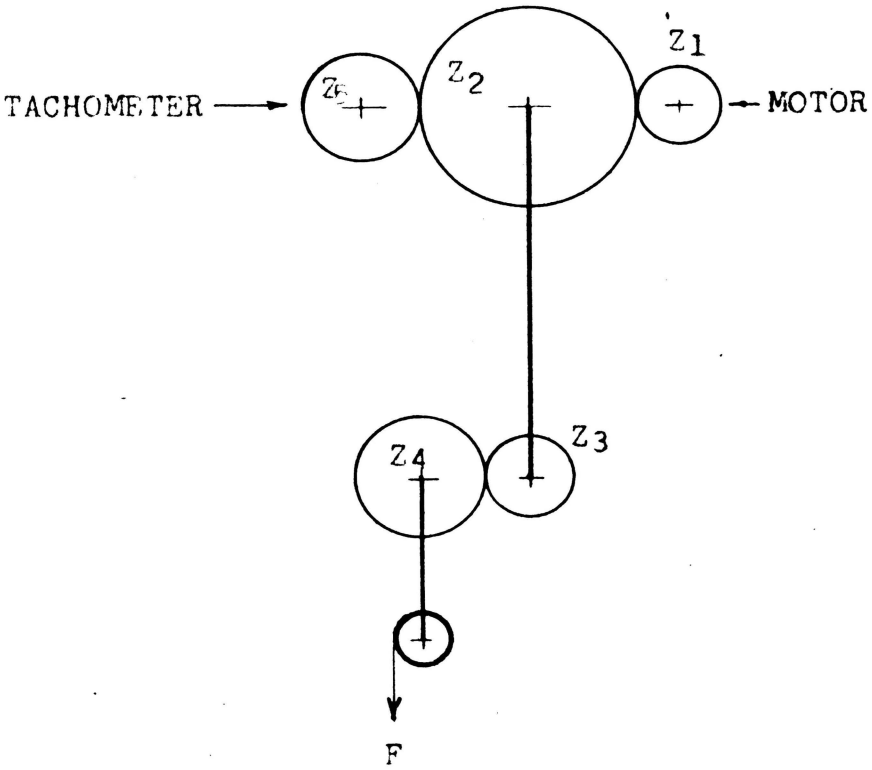

FIGURE 12

A-C SYSTEM GEAR TRAIN

and the dragging force of the tachometer. The steady state velocity is measured by recording the tachometer output as shown in Figure 13. The force F reduced to the motor shaft is

$$F_1 = F \frac{r}{r_4} \frac{r_3}{r_2}$$

the torque on the motor shaft

$$T_1 = Fr \frac{r_1}{r_4} \frac{r_3}{r_2}$$

the motor angular velocity

$$w_1 = w_5 \frac{r_5}{r_1}$$

Remembering that the radii of the wheels are proportional to the number of teeth, we obtain, after substituting the values of Z's given in Figure 12, and the following values

$$F = 200 \text{ gr.} = 7.06 \text{ oz.}$$

$$r = 0.75 \text{ in.}$$

$$w_5 = 400 \text{ rpm} = 42 \text{ rad/sec}$$

it can be shown that

$$T_1 = 7.06 \times 0.75 \times \frac{18}{72} \times \frac{23}{143} = 0.213 \text{ in-oz}$$

the motor angular velocity

$$w_1 = 42 \frac{54}{18} = 126 \text{ rad/sec}$$

By approximation, assuming that the friction constant reduced to motor shaft is

$$f_1 = \frac{T_1}{w_1} \cong 0.0005 \text{ in-oz.sec}$$

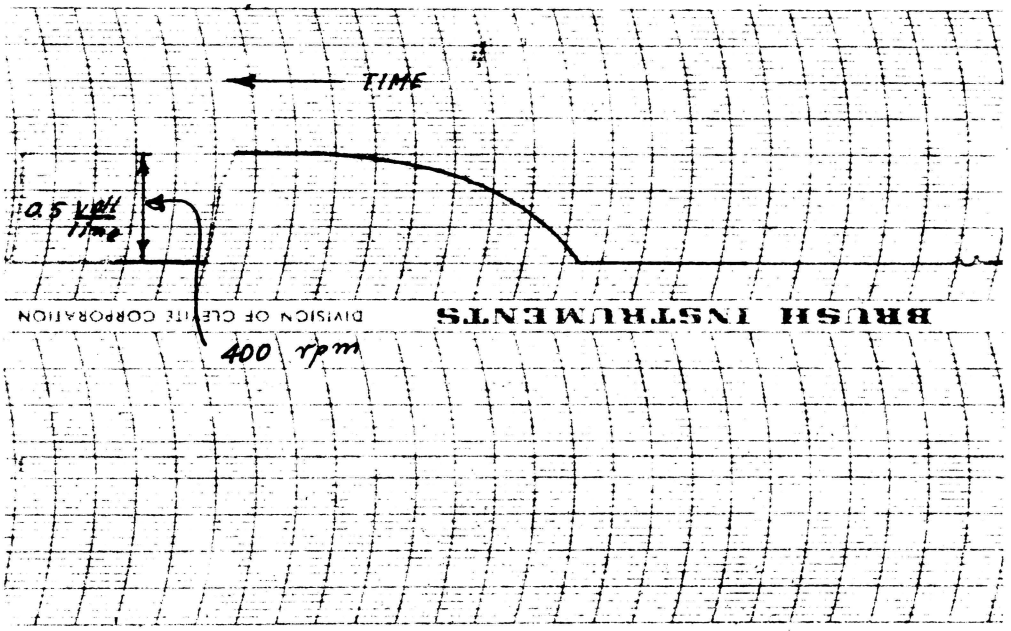

FIGURE 13

TACHOMETER RESPONSE FOR DETERMINING THE A-C SYSTEM FRICTION

The Motor Load Transfer Function [3,9,10,11,12]

The motor-load system consists of a 2-phase induction motor running a d-c tachometer through a gear train as shown in Figure 12-a. Knowing the motor speed torque characteristic, the motor torque constants can be determined, for 2 volt rms. applied to the control field. From Figure 11 and equation (10) we obtain

a) The motor damping constant

$$m = -\frac{\partial T}{\partial w} = \frac{T_{stall}}{w_{no\text{-}load}} = \frac{0.6}{600} \times \frac{60}{2\pi} = 0.0095 \text{ in-oz.sec.}$$

b) The motor torque constant

$$k = \frac{\partial T}{\partial V} = \frac{T_{stall}}{V_{applied}} = \frac{0.6}{2} = 0.3 \text{ in-oz/volt}$$

Equation (10) can be rewritten as

$$T + mw = kV \quad \ldots\ldots\ldots\ldots\ldots\ldots\ldots\ldots\ldots\ldots\ldots\ldots \quad (37)$$

Using Laplace transform, the motor-load differential equation would be given by

$$J p^2\theta + fp\theta = kV - mp\theta \quad \ldots\ldots\ldots\ldots\ldots\ldots\ldots\ldots \quad (38)$$

which is rearranged as follows:

$$\frac{\theta}{V} = \frac{k}{p(Jp + m + f)} \quad \ldots\ldots\ldots\ldots\ldots\ldots\ldots\ldots\ldots\ldots \quad (39)$$

or

$$\frac{\theta}{V} = \frac{k_m}{p(Tp + 1)} \quad \ldots\ldots\ldots\ldots\ldots\ldots\ldots\ldots\ldots\ldots \quad (40)$$

where

$$k_m = k/(m + f)$$

$$T = J/(m + f) \quad \ldots\ldots\ldots\ldots\ldots\ldots\ldots\ldots\ldots\ldots \quad (40a)$$

Substituting the known values, Equation (40a) becomes

$$k_m = \frac{0.3}{0.01} = 30 \text{ (volt-sec)}^{-1}$$

$$T = \frac{0.508 \times 10^{-3}}{0.01} = 0.508 \text{ sec.}$$

Substituting the above in Equation (40), the motor load transfer function is

$$\frac{\theta}{V} = \frac{30}{p(0.0508p + 1)} \quad \ldots\ldots\ldots\ldots\ldots\ldots \quad (41)$$

CHAPTER 2

GRAPHICAL DETERMINATION OF FREQUENCY RESPONSE[13]

Because of the difficulty in analysis of rotating components, magnetic amplifier, pneumatic and hydrodynamic systems, and the like, an analytic expression for the transfer function may be difficult to obtain. Determination of a component transfer function usually means determination of gain and phase relationship between the input and output signals to the particular component or system. Frequency-response data obtained experimentally present two problems: errors in measurement and unexpected factors in the transfer function, due to nonlinearities in the components' characteristics. Phase shift measurements, for example, are usually less accurate than attenuation measurements. On the other hand, the phase shift angle at the high-frequency end of the data is often greater than that expected from the attenuation characteristic by more that can be attributed to experimental error.

By making approximations with asymptotes to the actual response, a transfer function can be determined.

D-C SYSTEM

Description of System Tested

In order to take data for the frequency response and in the same time eliminate errors as much as possible, a simple position control system was built. The schematic diagram of this system is shown in Figure 14.

The principle components are:

1) Pair of synchros for detection of position errors of the output of the system.
2) Electronic Amplifier (Figure 17).
3) Amplidyne, to supply the command signal to the motor.
4) D-c shunt motor, the actuator unit.

Figure 15 is the block diagram of the control system. Figure 16 is the schematic setup for measuring the frequency response.

Principle of Operation

When an error input signal is given to the electronic amplifier while the amplidyne is rotating, a voltage will be built up, applied to the motor and an output shaft position will occur. by fixing a synchro generator rotor with 110 volts rms applied to it, a suppressed carrier amplitude modulated signal will occur at the control transformer rotor terminals.

A sinusoidal type of signal is generated by the function generator and applied to the input terminals of the electronic amplifier. By exciting the amplidyne with this amplified signal a voltage will be generated at the output terminals of the amplidyne and , applied to the motor. The motor will have a sinusoidal output motion.

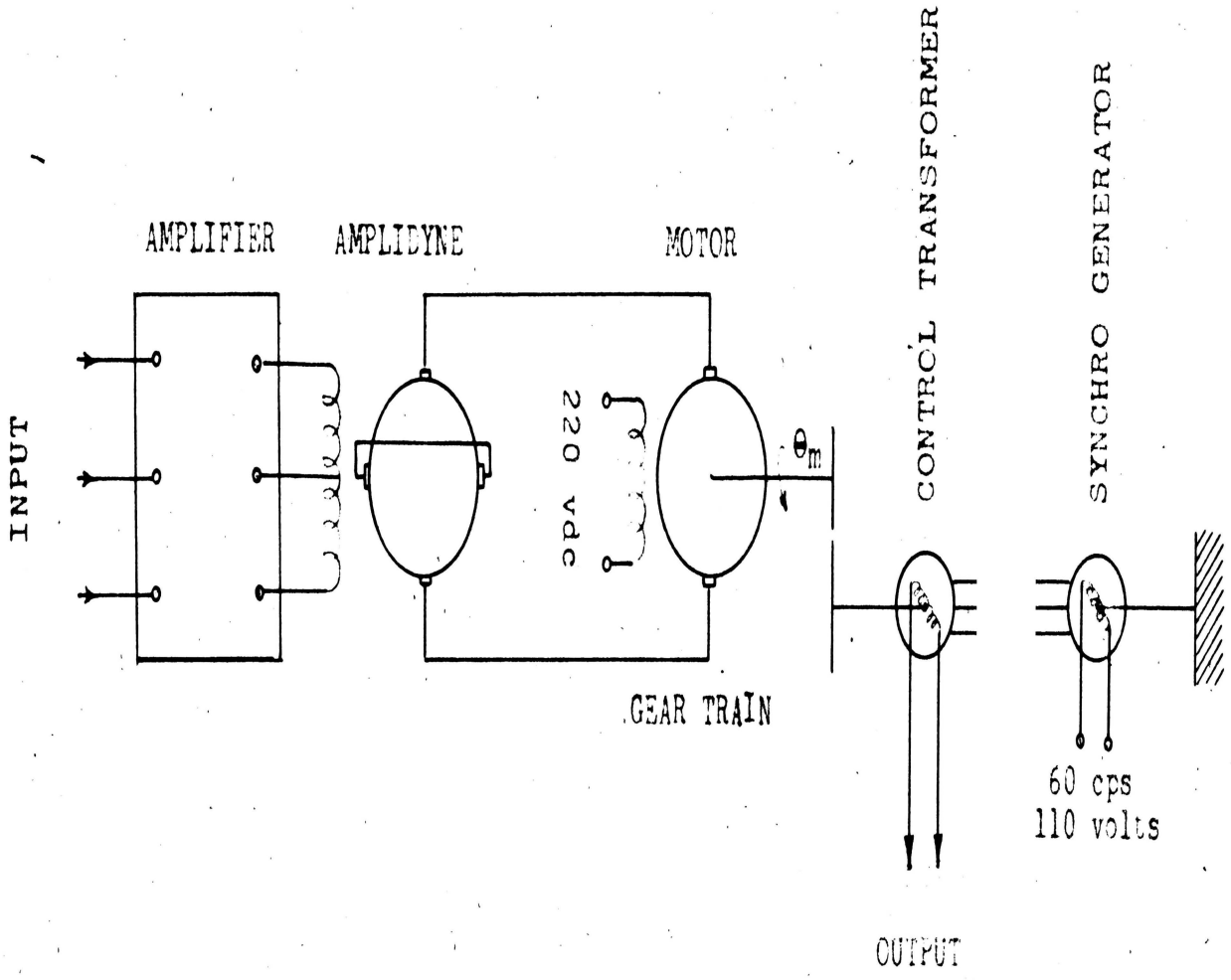

FIGURE 14

SCHEMATIC DIAGRAM OF D-C SYSTEM TESTED

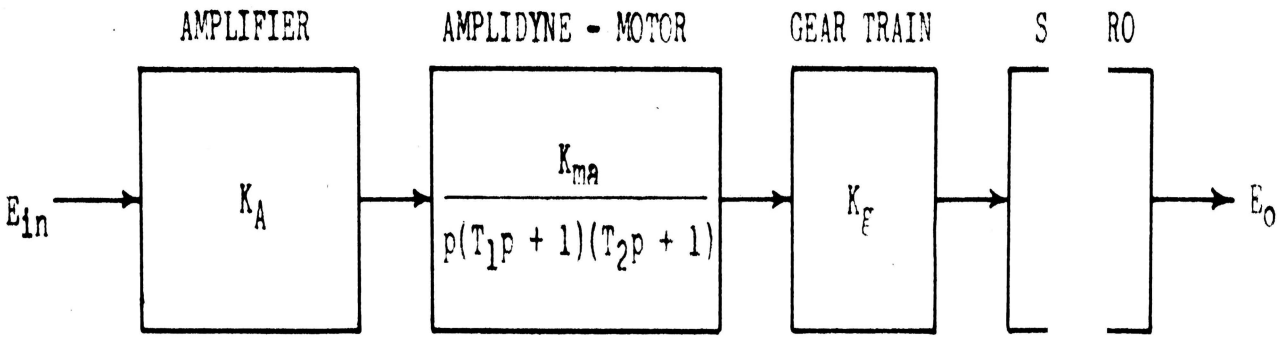

FIGURE 15

BLOCK DIAGRAM OF THE D-C SYSTEM

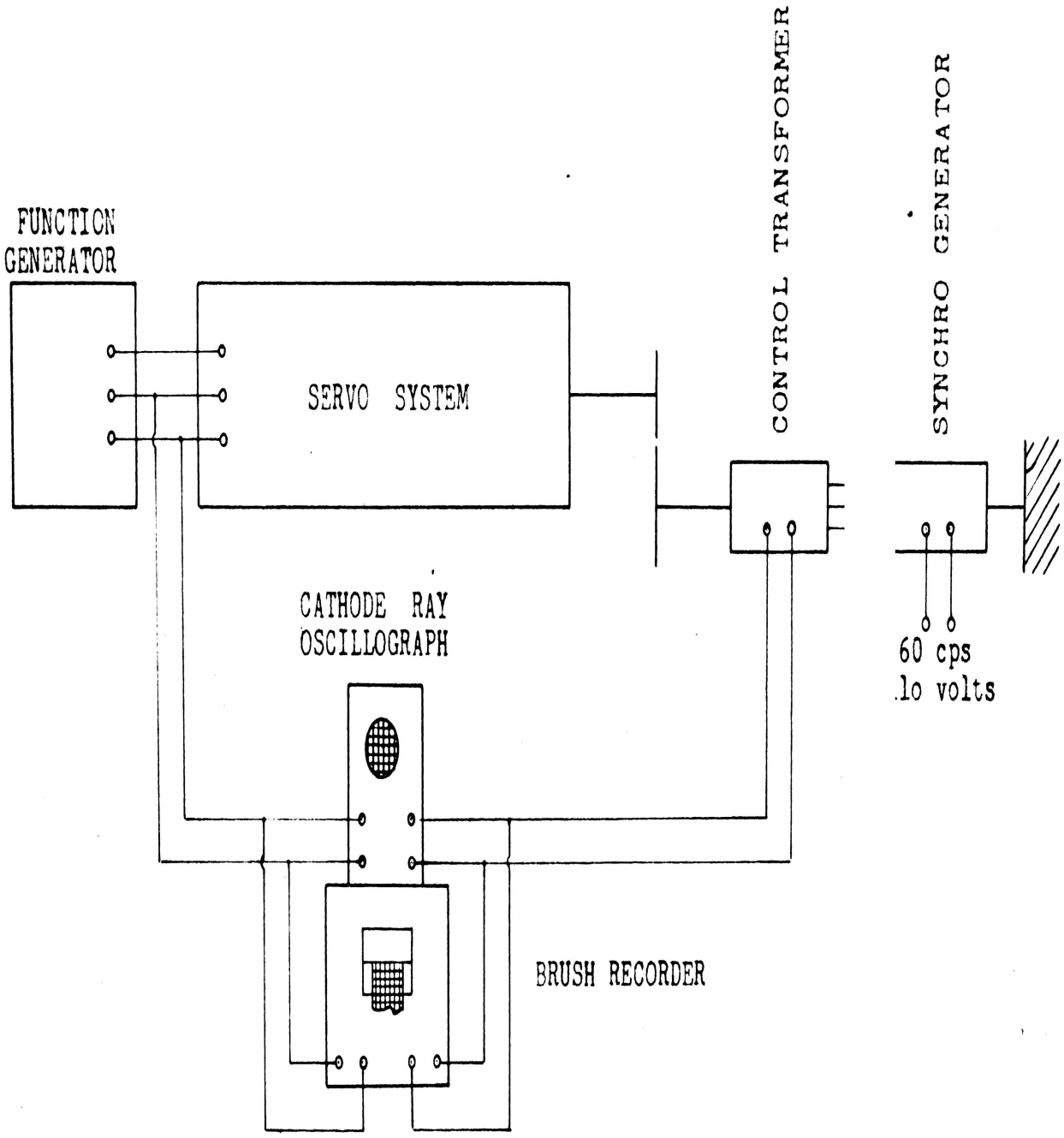

FIGURE 16

SCHEMATIC SETUP FOR MEASURING THE D-C SYSTEM FREQUENCY RESPONSE

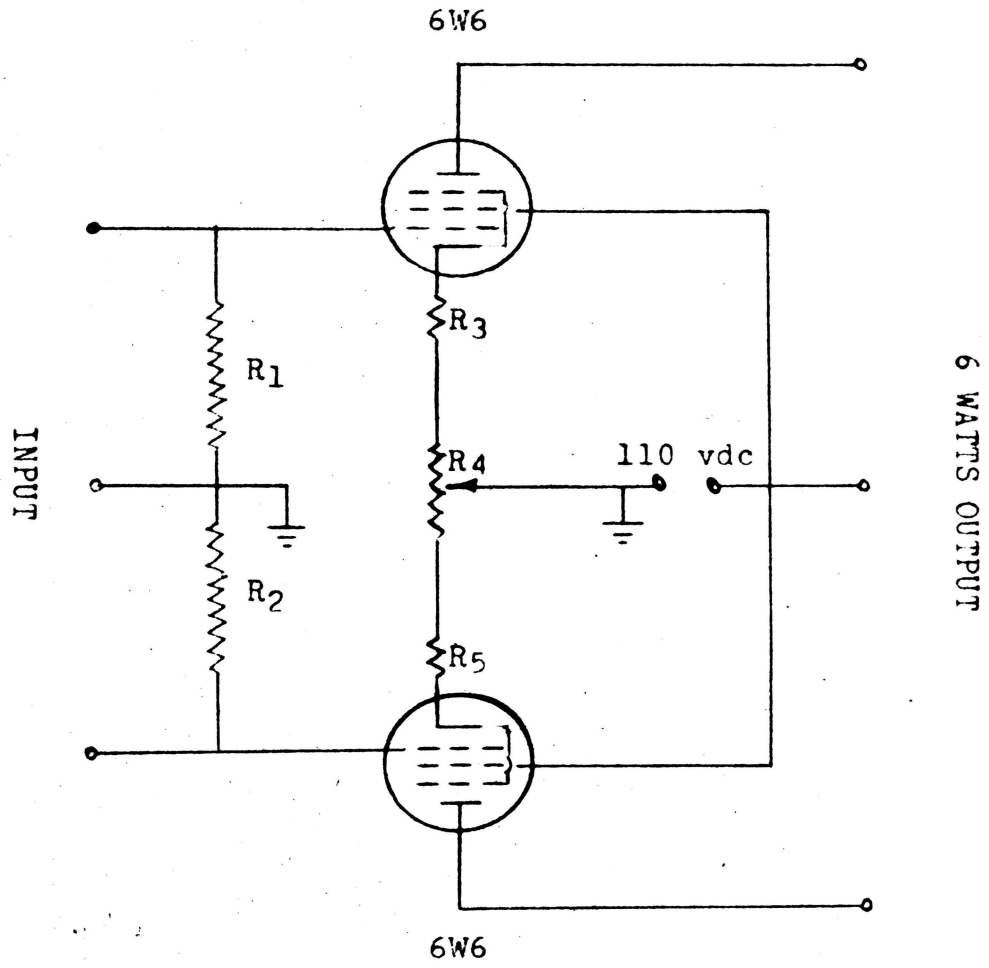

R_1 R_2 = 50000 ohms, 1 watt

R_3 R_5 = 270 ohms, 1 watt

R_4 = potentiometer, 100 ohms, 2 watts

FIGURE 17

D-C SYSTEM - SCHEMATIC DIAGRAM OF THE ELECTRONIC AMPLIFIER

The two signals are recorded by means of the Brush-Recorder, which has the advantage of recording two signals at the same time. A use of high persistance oscilloscope is recommended for checking wave forms before recording them, in order to have the wave form from which the phase shift and gain will easily be calculated, and a great deal of recording paper will be saved.

The unbalance of the amplidyne field which can be compensated by the electronic amplifier will cause a net rotation of the motor in one direction. This will appear on the recording paper by unsymmetrical wave form, a fact that has to be taken care of if more accurate results are needed. This is done by adjusting the cathode resistance.

Frequency Response from Experimental Data

The gain variation can be found by measuring the input and output voltages of the system. As for the phase shift, it can be determined by using the proper multiplying constant for the different frequencies. An example is shown in Figure 18. As it is shown, it is easier to measure the two peak-to-peak values of the signals, and calculate the gain; the phase lag in mm is measured between two peak points on the two wave forms. Care should be taken in measuring the phase shift in the low frequency range. Up to about 2 cycles per second the control transformer will have more than 180^{o} change in shaft position, and it will appear on the record as more than one cycle of output voltage for one cycle of input voltage.

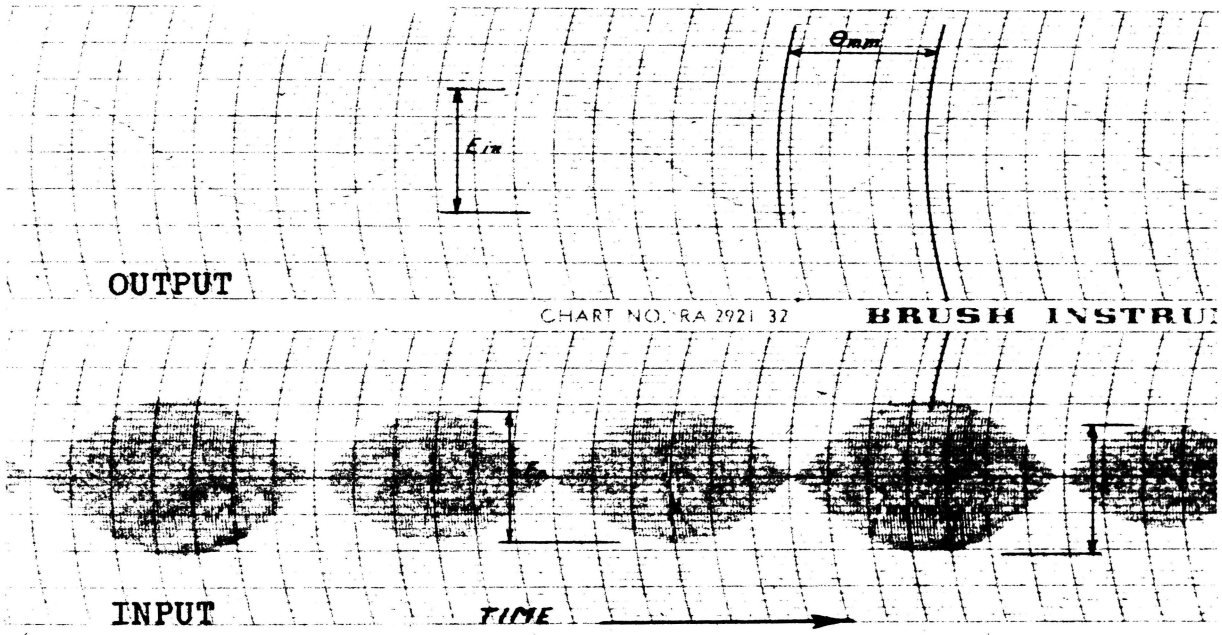

FIGURE 18

D-C SYSTEM - THE RECORDED INPUT AND OUTPUT SIGNALS

From Figure 18 we obtain:

Frequency (f): 0.4 c/sec

Chart velocity (ν): 25 mm/sec

Input signal (E_{in}): 17 mm = 17 x 0.2 = 3.4 volts

Output signal (E_o): 19 mm = 19 x 5 = 95 volts

Phase shift (θ): 19 mm = 109.6°

The constant multiplier for phase angle calculation is:

$$k = 360 \times f/\nu = 360 \times 0.4/25 = 5.76$$

the phase angle $\theta = 5.76 \times 19 = 109.6^{\circ}$

the gain $|KG| = E_o/E_{in} = 140/3.4 = 28$ volts/volt

Table V shows the calculated frequency response from the experimental data. Where

f, w - frequency

- recording chart speed

E_{in1} - scale used in recording input signal

E_{in2} - peak-to-peak value in mm of the input signal

E_{in3} - peak-to-peak value in volts of the input signal

E_{o1} - scale used in recording output signal

E_{o2} - peak-to-peak value in mm of the output signal

E_{o3} - peak-to-peak value in volts of the output signal

θ - phase angle (shift between output and input)

$|KG|$ - system gain

$\frac{|KG|}{K_A K_g K_s}$ - the amplidyne-motor gain

K_A - amplifier gain

K_g - gear ratio

K_s - synchro transfer function

TABLE V

D-C SYSTEM FREQUENCY RESPONSE - EXPERIMENTAL DATA

f c/sec	w sec^{-1}	mm/sec	E_{in} (1) v/mm	E_{in} (2) mm	E_{in} (3) volt	E_o (1) v/mm	E_o (2) mm	E_o (3) volt	θ mm	θ degre	|KG|	20logKG	$\frac{\|KG\|}{K_A K_g K_s}$
0.3	1.88	25	0.2	17	3.4	5.00	25.0	125.0	23	-100	,800	31.4	19.80
0.4	2.51	25	0.2	17	3.4	5.00	19.0	95.0	19	-109	,000	28.9	15.00
0.6	3.77	25	0.2	17	3.4	5.00	12.0	60.0	14	-121	,600	25.0	9.45
0.8	5.02	25	0.2	17	3.4	2.00	24.0	48.0	11	-127	,800	23.0	7.40
1.1	6.90	25	0.2	17	3.4	2.00	17.5	35.0	8	-135	,300	20.3	5.54
1.5	9.40	125	0.1	32	3.2	1.00	24.0	24.0	34	-149	500	17.5	2.64
2.0	12.55	125	0.2	17	3.4	1.00	20.0	20.0	29	-168	,900	15.4	2.08
3.0	18.80	125	0.2	17	3.4	0.50	21.0	10.5	22	-185	100	9.8	1.09
4.0	25.10	125	0.2	19	3.8	0.50	14.0	7.0	18	-198	840	5.3	0.64
5.0	31.40	125	0.2	19	3.8	0.20	18.0	3.6	15	-216	950	- 0.5	0.33
6.0	37.70	125	0.2	21	4.2	0.20	15.0	3.0	13	-225	715	- 2.9	0.25
7.0	44.00	125	0.2	23	4.6	0.20	13.0	2.6	12	-242	565	- 4.9	0.19
9.0	56.50	125	0.2	23	4.6	0.20	6.0	1.2	10	-255	261	-11.7	0.09
10.0	62.80	125	0.2	32	6.4	0.05	15.0	1.2	9	-260	195	-14.2	0.07

Table VI shows the calculated frequency response from the theoretical transfer function, equation (35) on page 22.

Transfer Function from Frequency Response

Figure 19 shows the actual frequency response of the d-c system. Fitting series of straight lines as asymptotes will determine the corner frequencies. In Figure 19, two straight lines are fitted with a double corner frequency at

$$w = 27 \text{ rad/sec.}$$

this gives the two time constants of the overall transfer function. In order to obtain the transfer function of the amplidyne-motor set, the overall transfer function was divided by the gain of the amplifier, the gear ratio and the gain of the synchro.

a) The amplifier gain is

$$K_A = 2.86 \text{ ma/volt}$$

b) The gear ratio (Figure 20)

$$K_g = 1/60$$

c) For the synchro, two different gain constants were used: One for the high frequencies, and one for the low frequencies. The reason for that is the fact that for low frequencies the control transformer has a larger change in shaft position compared to that for high frequencies. The two gains are chosen from Figure 21 on page 49.

(Low frequencies) $K_{s1} = 39$ volts/rad

(High frequencies) $K_{s2} = 59$ volts/rad

A new asymptotic approximation to the frequency response is

TABLE VI

D-C SYSTEM FREQUENCY RESPONSE - THEORETICAL DATA

f c/sec	w sec^{-1}	0.0775w	$\|0.0775wj + 1\|$	$\|0.0775wj + 1\|^2$	θ degree	$\|KG\|$	$20\log\|KG\|$
0.3	1.88	0.146	1.010	1.020	-106.3	18.800	25.5
0.4	2.51	0.195	1.021	1.042	-112.0	13.800	22.8
0.6	3.77	0.292	1.040	1.081	-122.6	8.860	19.0
0.8	5.02	0.389	1.071	1.148	-132.6	6.270	15.9
1.1	6.90	0.535	1.136	1.290	-146.2	4.060	12.1
1.5	9.40	0.730	1.238	1.533	-162.4	2.500	8.0
2.0	12.55	0.974	1.396	1.950	-178.4	1.476	3.4
3.0	18.80	1.460	1.770	3.130	-201.2	0.613	- 4.2
4.0	25.10	1.950	2.290	5.240	-215.6	0.275	-11.2
5.0	31.40	2.430	2.625	6.860	-225.2	0.167	-15.5
6.0	37.70	2.920	3.090	9.550	-232.2	0.100	-20.0
7.0	44.00	3.410	3.565	12.700	-236.4	0.064	-23.8

obtained in Figure 19, after subtracting the proper gains, (a), (b), and (c). This is the frequency response of the amplidyne-motor set, and the transfer function is of the form

$$\frac{K_{ma}}{p(Tp + 1)^2} \quad \ldots\ldots\ldots\ldots\ldots\ldots\ldots\ldots \quad (42)$$

where $K_{ma} = \dfrac{K}{K_A K_g K_s}$

substitute the values

$$T = \frac{1}{22} = 0.0455 \text{ sec.}$$

$$K_{ma} = 38$$

and the amplidyne-motor transfer function is

$$\frac{38}{p(0.0455p + 1)^2} \quad \ldots\ldots\ldots\ldots\ldots\ldots\ldots\ldots \quad (43)$$

Plotting the variation of the phase shift with frequency as given in Table VII (page 46) in Figure 19, shows how close this compares with the measured phase shift. Figure 22 is a polar plot of the frequency response obtained analytically and experimentally. Figure 23 is the high-frequency portion of the frequency response. A negative phase margin is seen, which has to be taken care of by means of compensation for a stable closed-loop control system. The comparison of the analytical and the experimental frequency response is given also in Figure 24 on page 52.

TABLE VII

PHASE SHIFT VARIATION OF DETERMINED TRANSFER FUNCTION

w sec^{-1}	$0.0455w$	$\angle (0.0455jw + 1)$ degree	$\angle \frac{1}{jw(0.0455jw + 1)^2}$ degree
3	0.131	7.5	-105
5	0.228	13.0	-116
7	0.138	17.5	-125
10	0.412	22.5	-135
15	0.682	34.0	-158
20	0.912	42.5	-175
30	1.310	52.5	-195
50	2.280	66.5	-223
70	3.180	72.5	-235

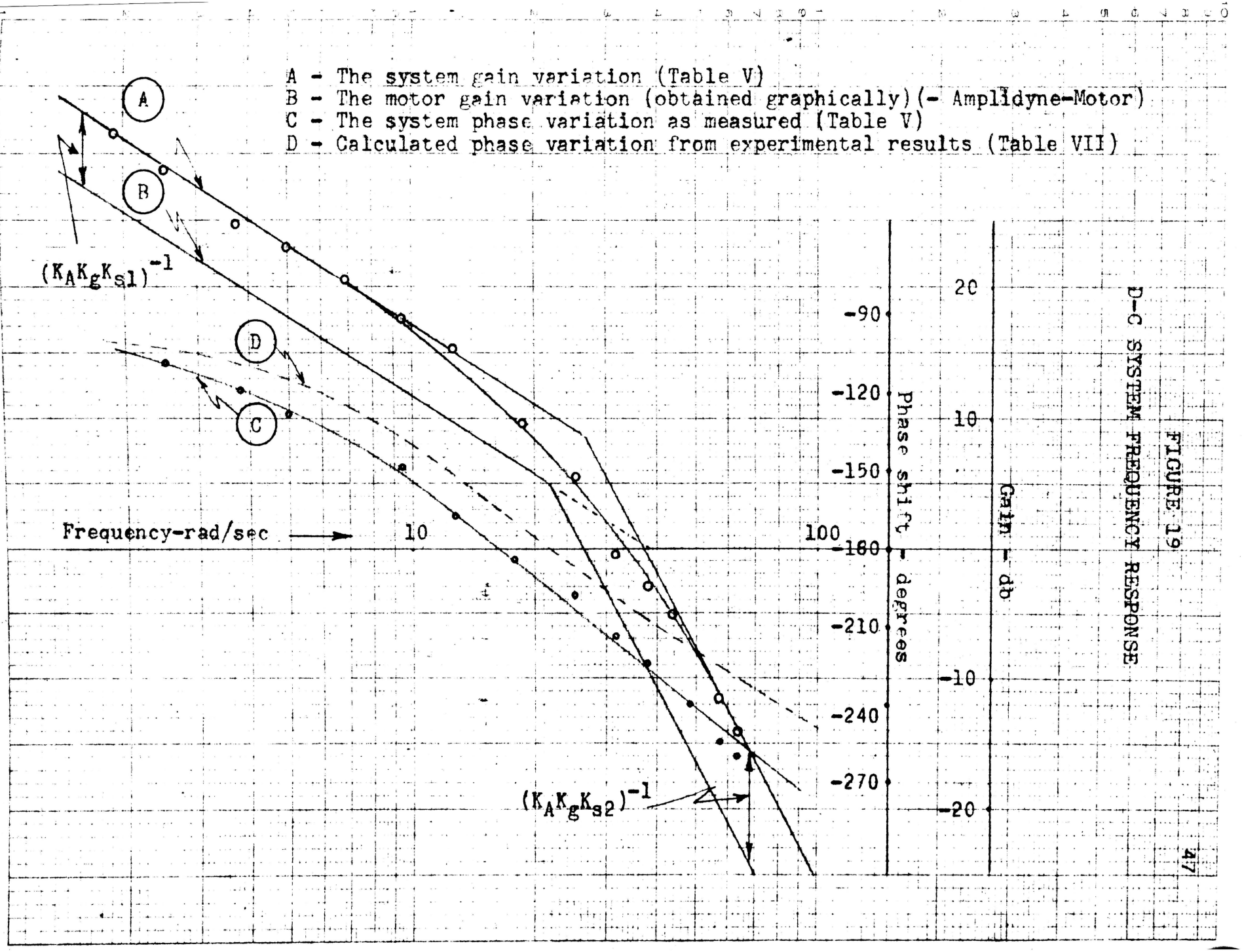

FIGURE 19 D-C SYSTEM FREQUENCY RESPONSE

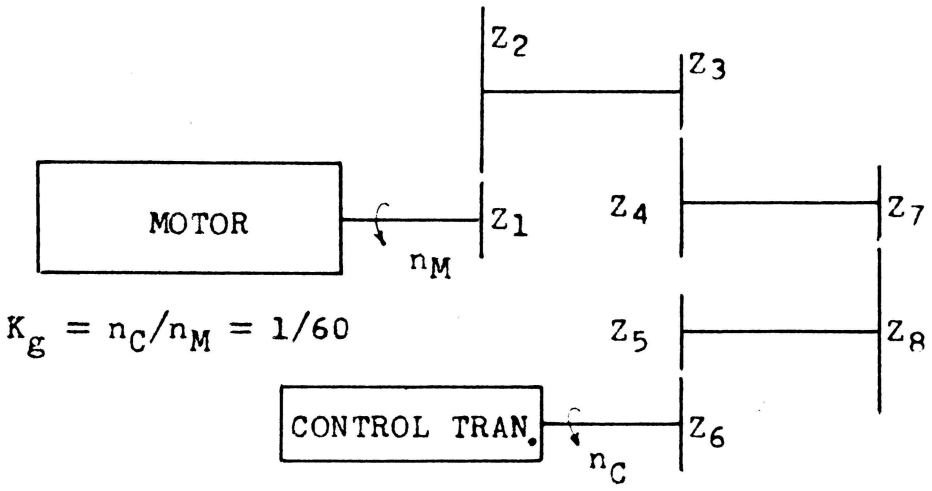

Z_1 = 28 Teeth
Z_2 = 130 "
Z_3 = 20 "
Z_4 = 58 "
Z_5 = 32 "
Z_6 = 35 "
Z_7 = 20 "
Z_8 = 82 "

FIGURE 20

D-C SYSTEM GEAR TRAIN

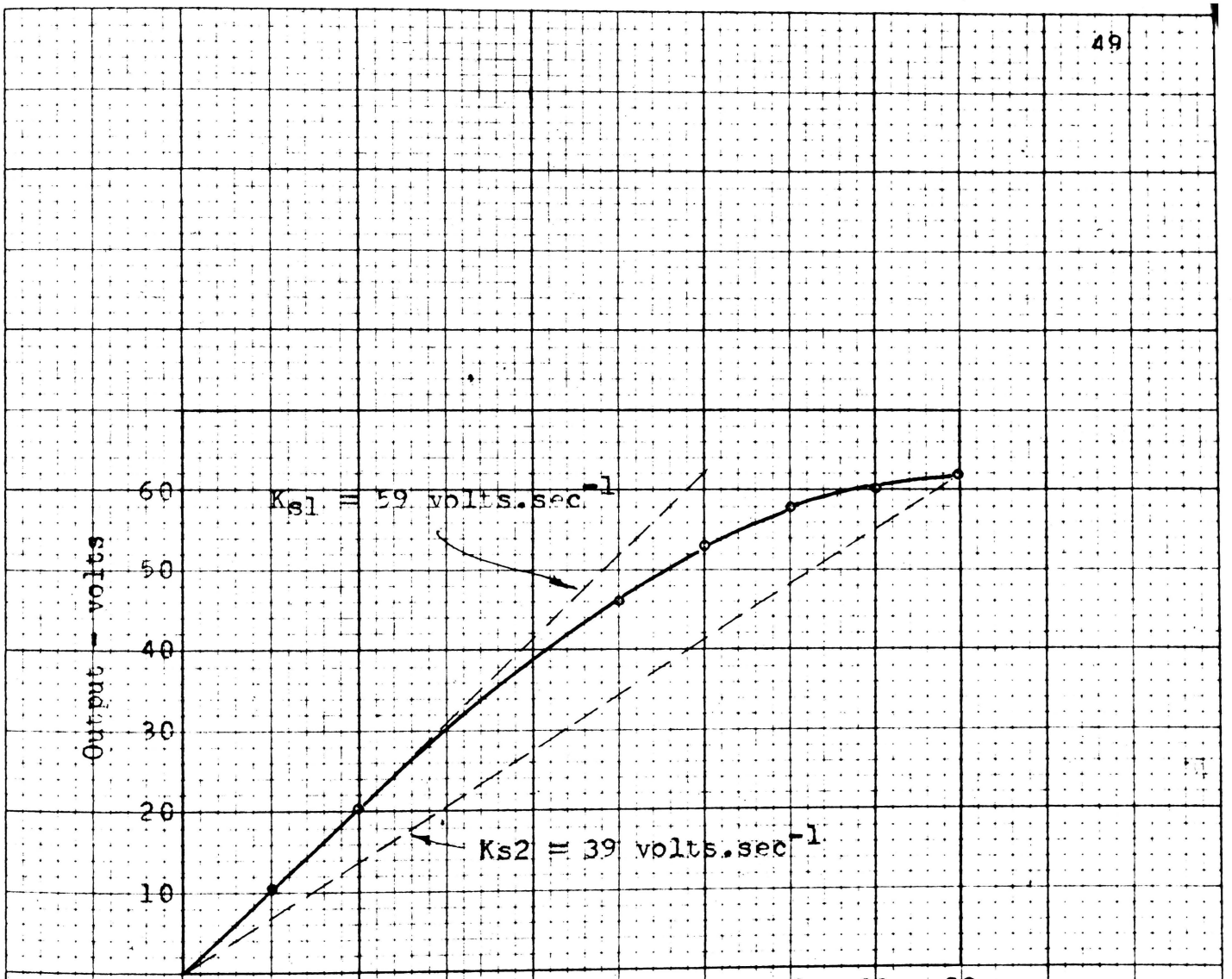

FIGURE 21

D-C SYSTEM - CONTROL TRANSFORMER CHARACTERISTIC

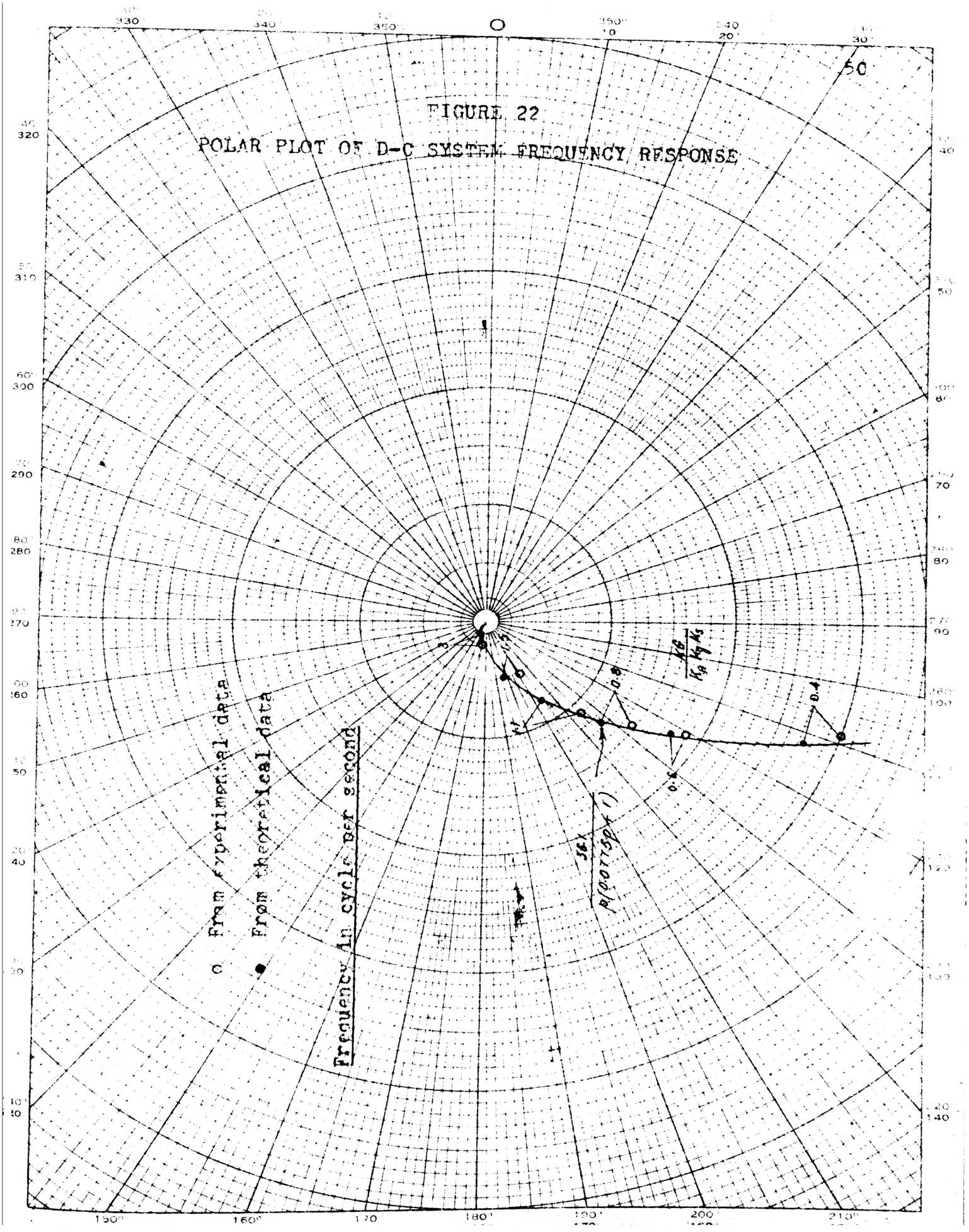
FIGURE 22
POLAR PLOT OF D-C SYSTEM FREQUENCY RESPONSE
50
o From experimental data
• From theoretical data
Frequency in cycles per second
0.8
0.4
0.2

FIGURE 23

HIGH FREAUENCY PORTION OF THE POLAR PLOT OF THE D-C SYSTEM

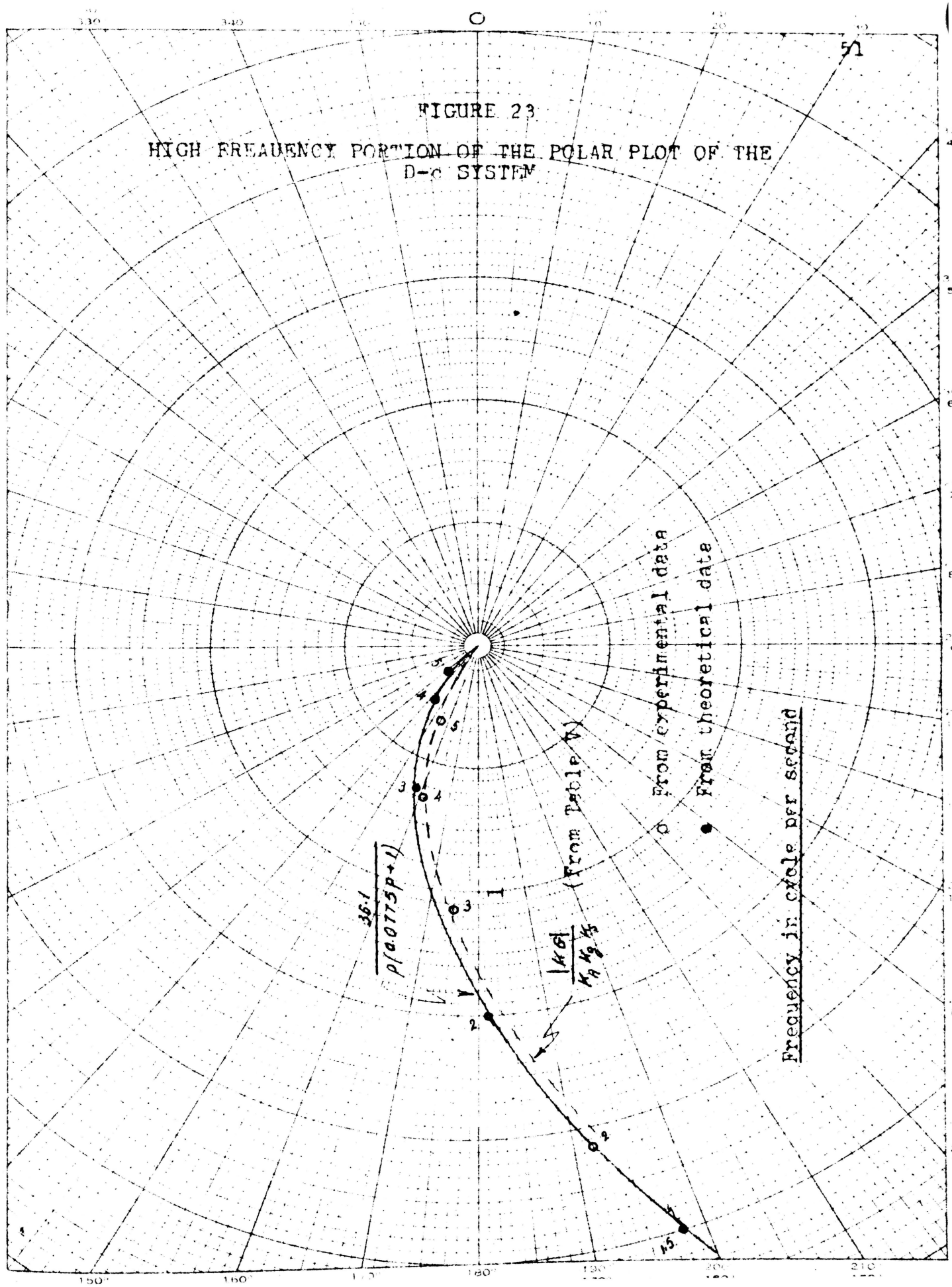

FIGURE 24

COMPARISON OF ANALYTICALLY AND EXPERIMENTALLY OBTAINED D-C SYSTEM FREQUENCY RESPONSE

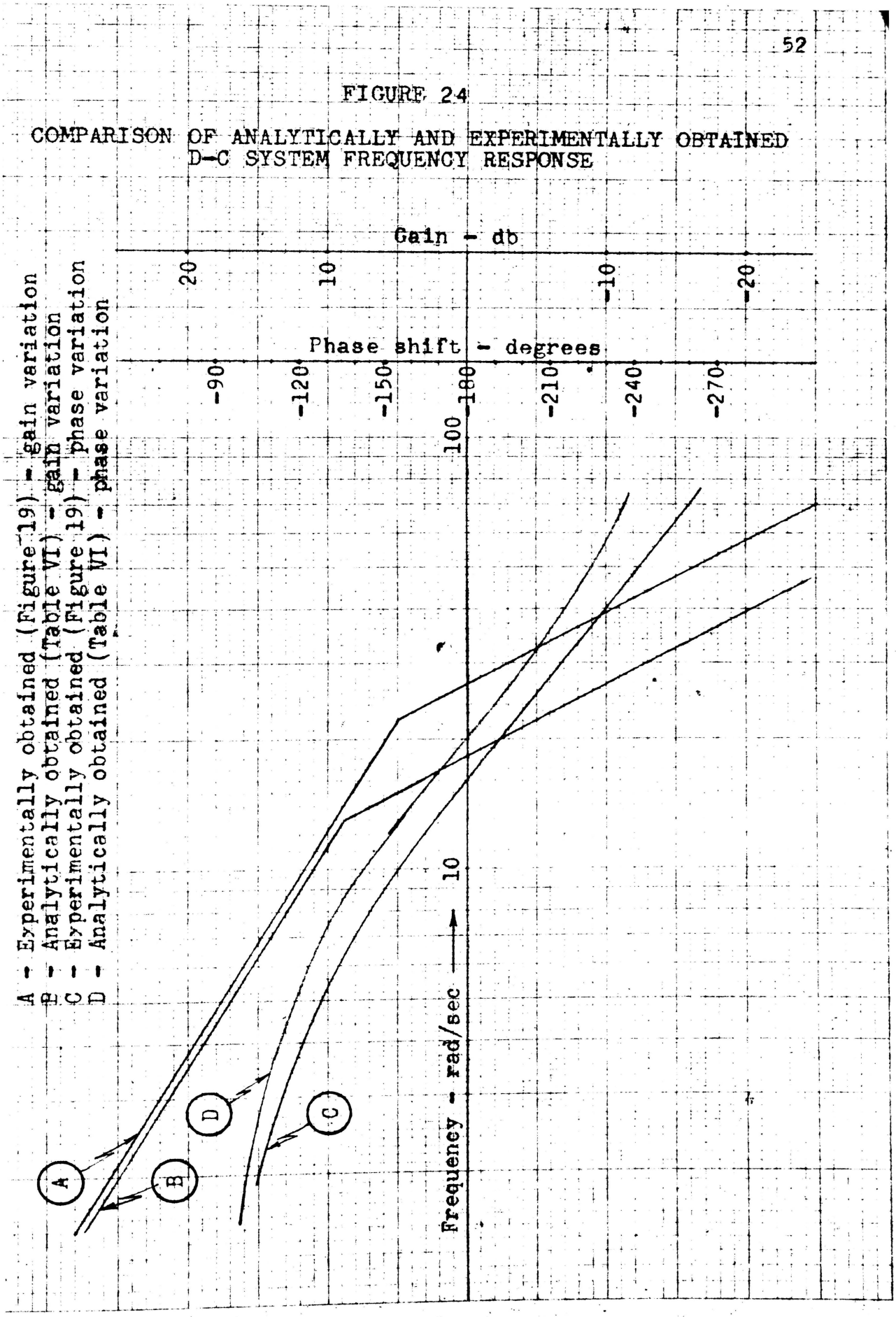

A-C SYSTEM

Description of System Tested

The system designed consists of the following main components (Figure 25, page 58).

1) A pair of synchros for generating a modulated carrier signal
2) Electronic amplifier to amplify the input signal (Figure 28, page 61,62)
3) 2-phase induction motor of which the fixed phase is excited by 60 cps, 20 volts rms
4) A d-c tachometer as the output measuring device of the system

The block diagram in Figure 26 shows the system components as far as the overall transfer function is concerned. Figure 27 is the schematic set-up for measuring the frequency response.

Principle of Operation (Figures 25,26,27)

A d-c motor turning an excited synchro generator will cause a sinusoidal modulated signal to appear between the generator fixed phase terminals. The voltage is induced in the control transformer variable phase which was applied to the system input terminals. An amplifier amplified the signal and applied it to the control phase of the a-c motor. A tachometer, coupled to the motor through a gear train gave an indication of the output shaft variation (tachometer constant is 2 volts/100 rpm).

The phase shift between the control phase voltage and the reference phase voltage was adjusted to 90°, by means

of the phase shifter (Figure 28a, page 61)

After applying voltage to the d-c motor the calibrated dial was adjusted to indicate zero degrees, for minimum phase shift of the modulating signal between the fixed and the variable phase of the control transformer. Variation of the modulating frequency was made by varying the speed of the d-c motor. The a-c motor oscillated back and forth due to the fact that the sign of the control signal depends on the polarity of the carrier signal. In the region where the signal amplitude approaches the origin, (Point A on Figure 29, page 63), the carrier signal reverses polarity. As a consequence, the tachometer output is of a sine wave form.

The input and output signal to the system were recorded by means of the Brush-Recorder, and the gain and phase shift were determined using the same method that was described before.

For the high-frequency range the phase shift was determined by adjusting the variable phase position of the control transformer to give zero phase shift pattern on the scope (Figure 30, page 64). For low-frequency operation, the frequency was determined from the recorder chart, and for high-frequency by knowing the constant of the integrally mounted tachometer on the d-c motor, which was found to be 1.6 volts per cycle per second.

Frequency Response from Experimental Data

The phase shift and the gain variation were calculated from the recorded information and tabulated in Table VIII. The amplifier frequency response data were measured in the same method and tabulated in Table IX.

The system and amplifier frequency response are given in Figure 31 on page 65. In order to obtain the motor frequency response for the purpose of determining its transfer function, the amplifier response was subtracted from the overall system response for the gain as well as for the phase, Figure 31 and 32.

Figure 33 on page 67 shows how the motor frequency response was determined by subtracting the tachometer and the gear train transfer function from KG/K_A. From Figure 33 it is easily seen that the transfer function of the motor is

$$\frac{45}{p(0.0333p + 1)} \quad \ldots\ldots\ldots\ldots\ldots \quad (44)$$

Figure 34 on page 68 is the comparison between analytical and experimental results.

TABLE VIII

A-C SYSTEM FREQUENCY RESPONSE - EXPERIMENTAL DATA

ω sec^{-1}	E_{in} volt	E_o volt	θ degree	|KG|	20log |KG|
0.70	8.50	22.0	3	2.60	8.30
1.32	8.50	22.0	- 10	2.60	8.30
1.92	8.25	22.0	- 14	2.60	8.30
3.00	8.25	22.0	- 20	2.60	8.30
6.28	8.00	22.0	- 37	2.60	8.30
13.50	6.80	19.0	- 62	2.50	8.00
19.50	6.80	16.0	- 75	2.33	7.00
26.20	6.80	13.0	- 85	1.90	5.56
34.10	6.80	10.5	-100	1.55	3.80
39.20	6.80	9.0	-110	1.33	2.48
49.00	6.80	7.4	-120	1.09	0.80
59.00	6.80	6.0	-130	0.88	-1.20
70.40	6.60	4.4	-147	0.67	-3.50
84.00	6.40	4.0	-160	0.60	-4.40
100.00	6.20	3.0	-172	0.48	-6.30

TABLE IX

THE AMPLIFIER FREQUENCY RESPONSE DATA

w rad/sec	gain K_A	θ degree	$20\log K_A$
0.523	2.74	0	8.75
1.54	2.74	0	8.75
2.04	2.74	- 5	8.75
6.53	2.74	-10	8.75
13.50	2.66	-25	8.43
20.70	2.48	-30	7.90
29.10	2.48	-36	7.90
39.20	2.28	-44	7.16
60.30	2.10	-60	6.45

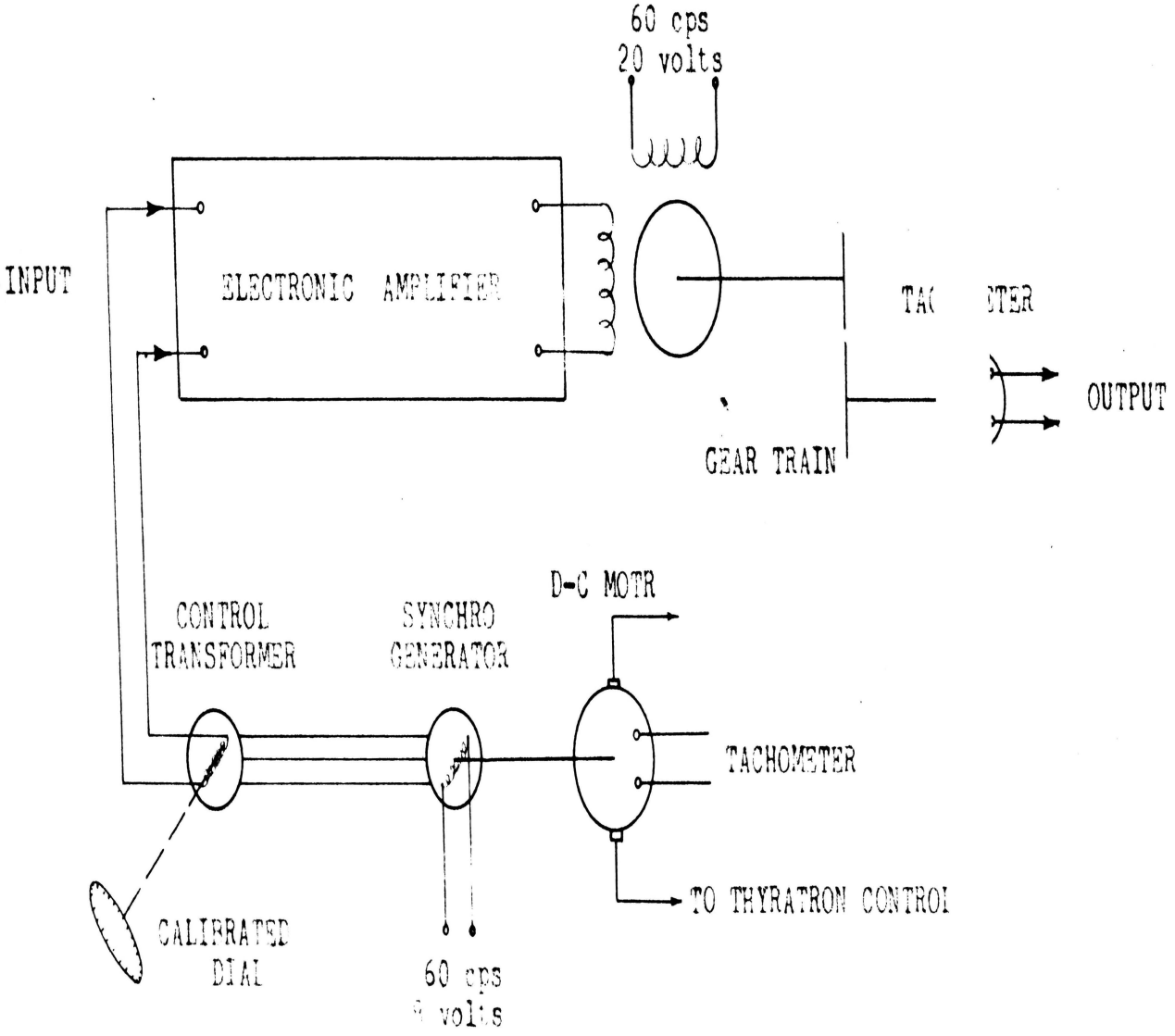

FIGURE 25

SCHEMATIC DIAGRAM OF A-C SYSTEM TESTED

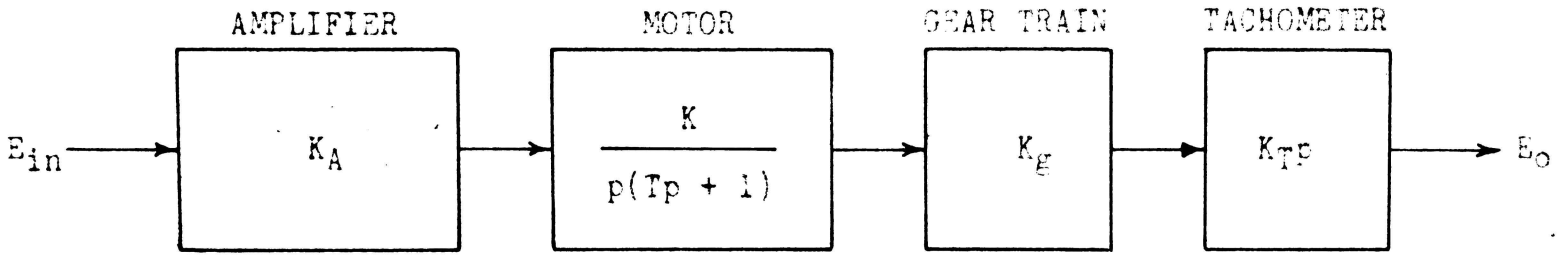

FIGURE 26

BLOCK DIAGRAM OF THE A-C SYSTEM

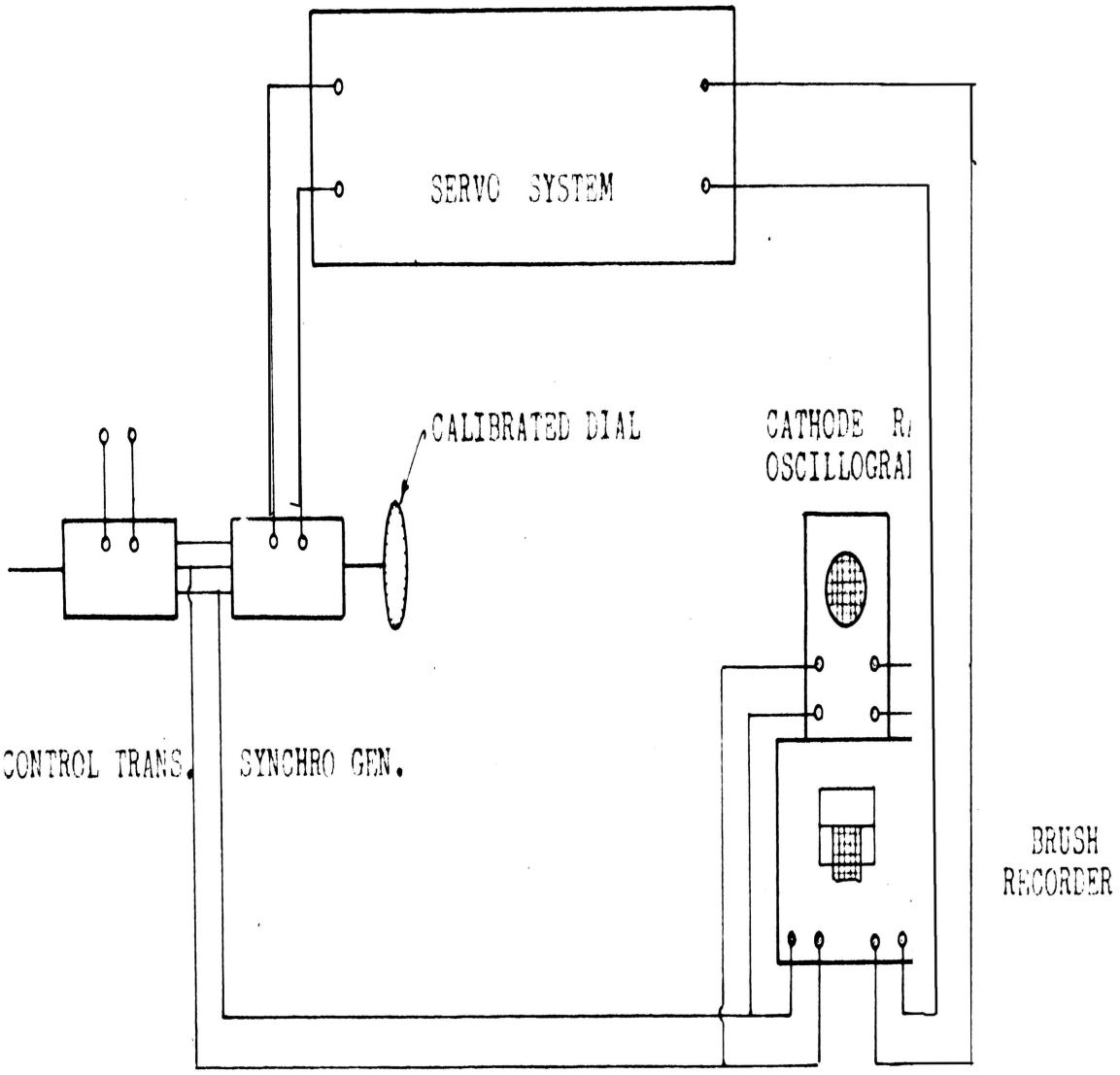

FIGURE 27

SCHEMATIC SETUP FOR MEASURING THE A-C SYSTEM FREQUENCY RESPONSE

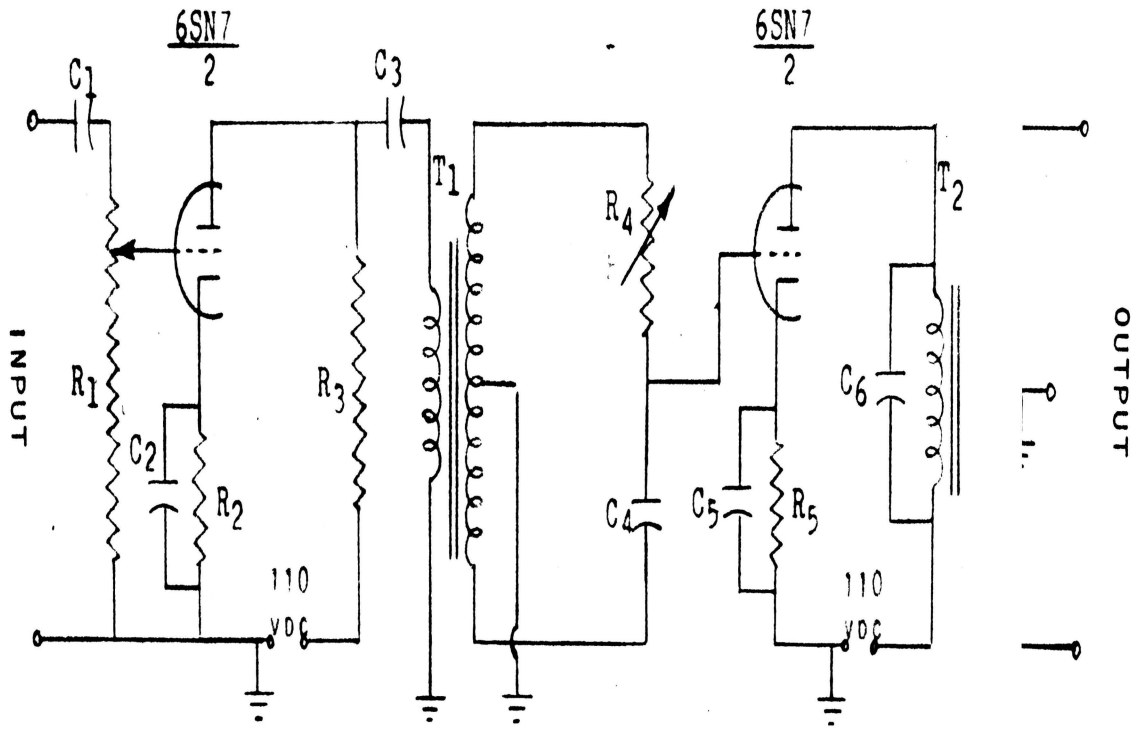

C_1 = 0.005 MFD, paper, 400 VDC
C_2 C_5 = 30 MFD, paper, 150 VDC
C_3 C_4 = 0.25 MFD, paper, 400 VDC
C_6 = 0.1 MFD, paper, 400 VDC

R_1 = 100000 ohms, potentiometer
R_2 R_5 = 850 ohms, 5 watts
R_3 = 7500 ohms, 1watt
R_4 = 0.1 megohm, potentiometer

T_1 = Interstage transformer, pri. to sec. ratio 3:1
T_2 = Driver transformer, pri. to sec. ratio 2.5:1

FIGURE 28(a)

A-C SYSTEM - SCHEMATIC DIAGRAM OF THE VOLTAGE AMPLIFIER

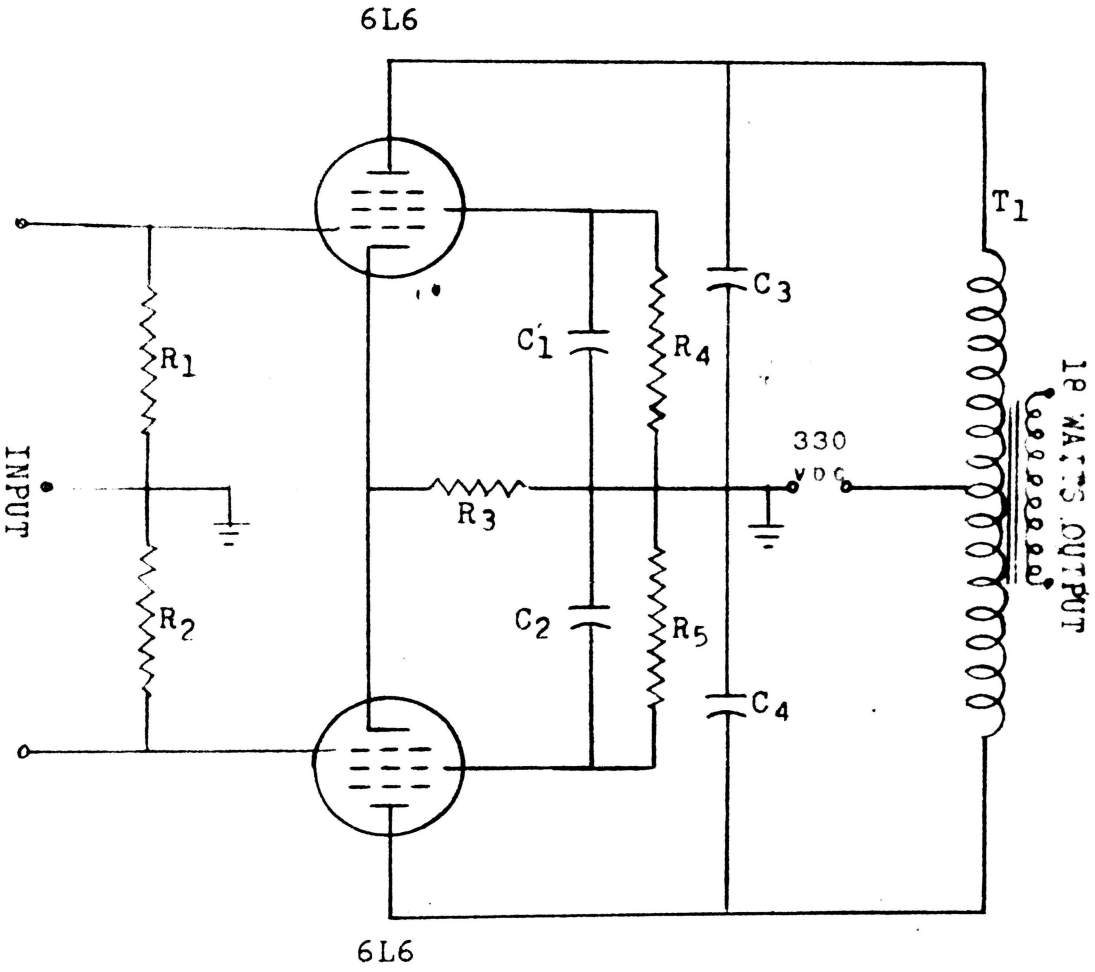

C_1 C_2 = 0.05 MFD, paper, 400 volts
C_3 C_4 = o.5 MFD, paper, 400 volts

R_1 R_2 = 200000 ohms, 1 watt
R_3 = 250 ohms, 10 watts
R_4 R_5 = 15000 ohms, 2 watts

T_1 = Output transformer for matching control field of 2-phase a-c motor impedance to 6000-ohm tube load

FIGURE 28(b)

A-C SYSTEM - SCHEMATIC DIAGRAM OF THE POWER AMPLIFIER

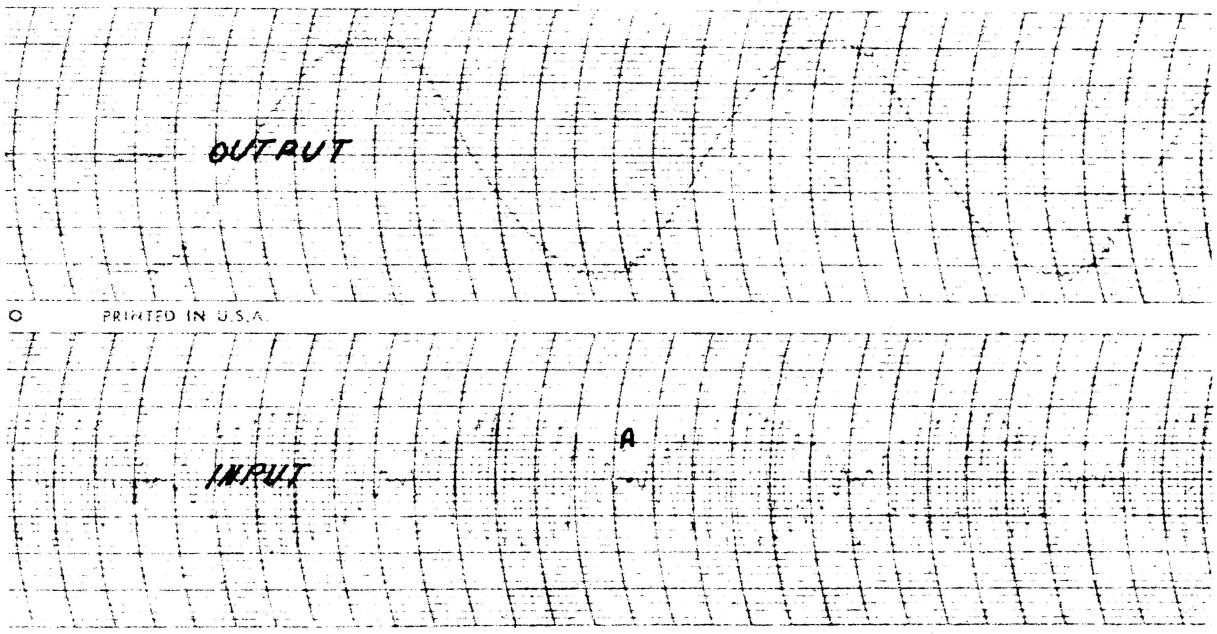

FIGURE 29

A-C SYSTEM - THE RECORDED INPUT AND OUTPUT SIGNALS

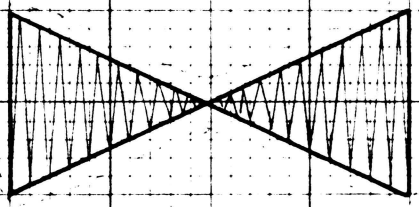

0° shift

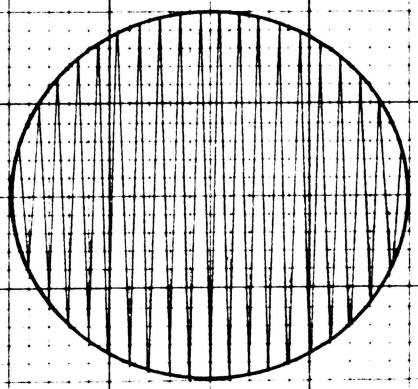

90° shift

FIGURE 30

SCOPE PETTERNS FOR DETERMINING PHASE SHIFT IN A-C SYSTEM

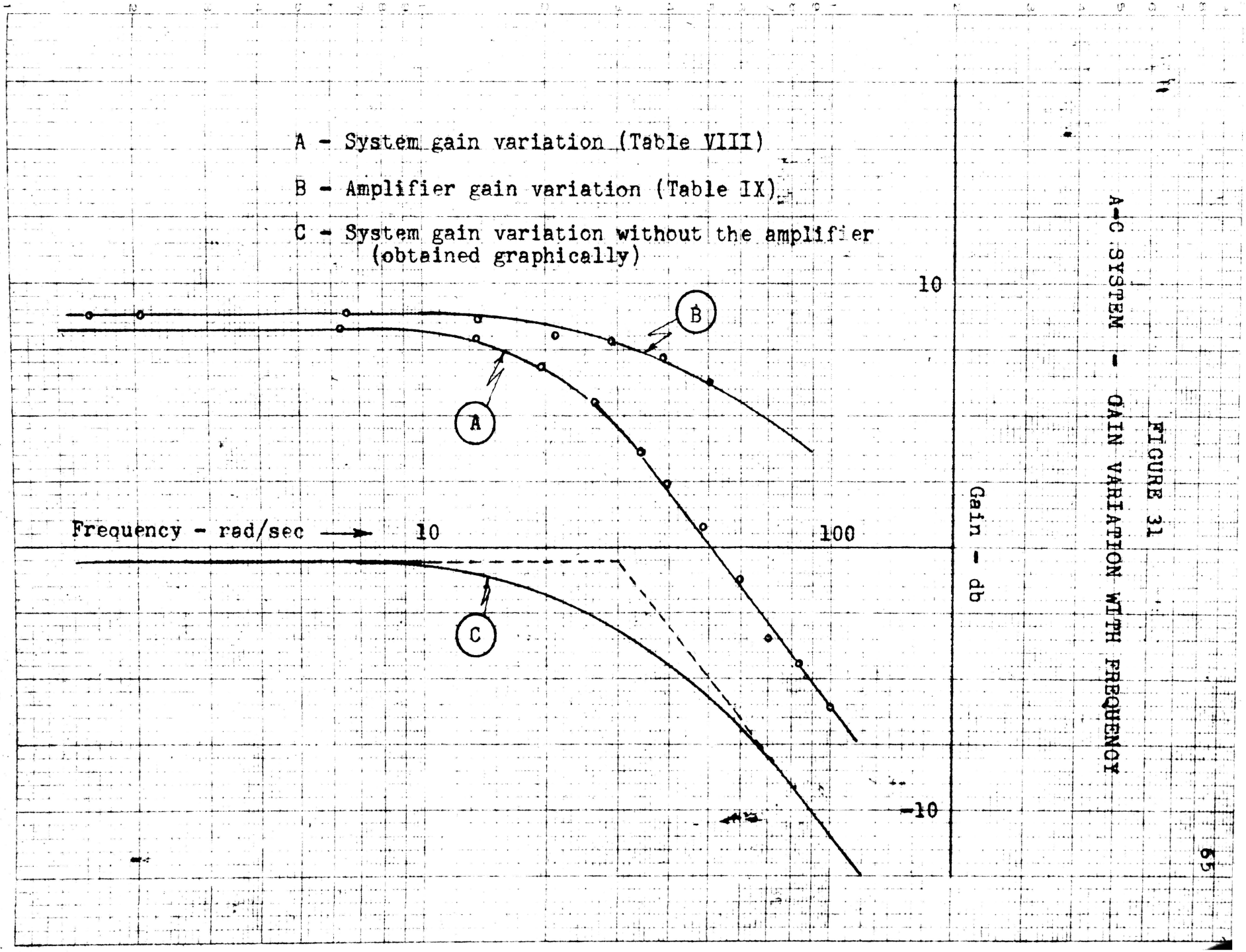

FIGURE 31

A-C SYSTEM - GAIN VARIATION WITH FREQUENCY

FIGURE 32

A-C SYSTEM - PHASE VARIATION WITH FREQUENCY

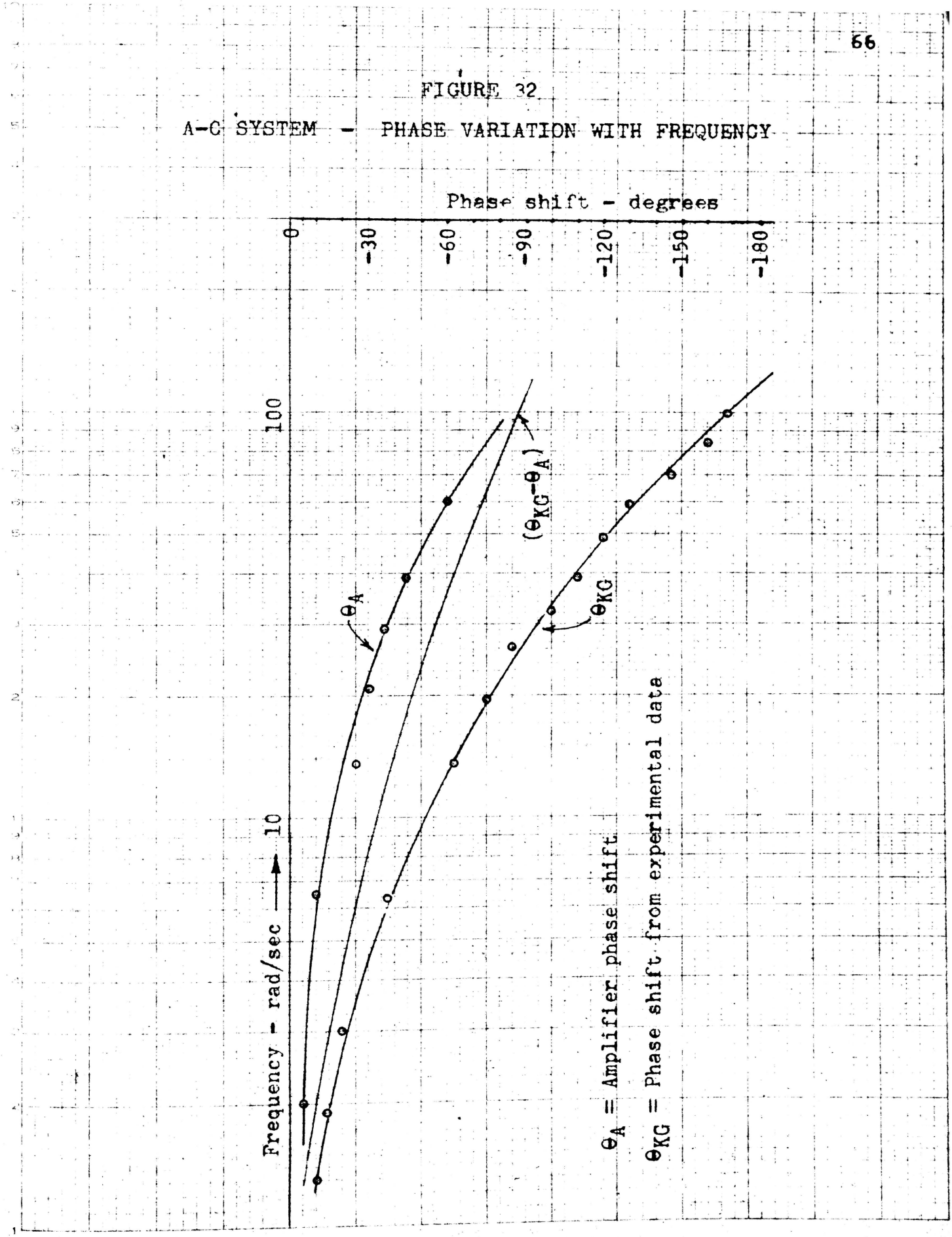

FIGURE 33

DETERMINATION OF A-C MOTOR FREQUENCY RESPONSE

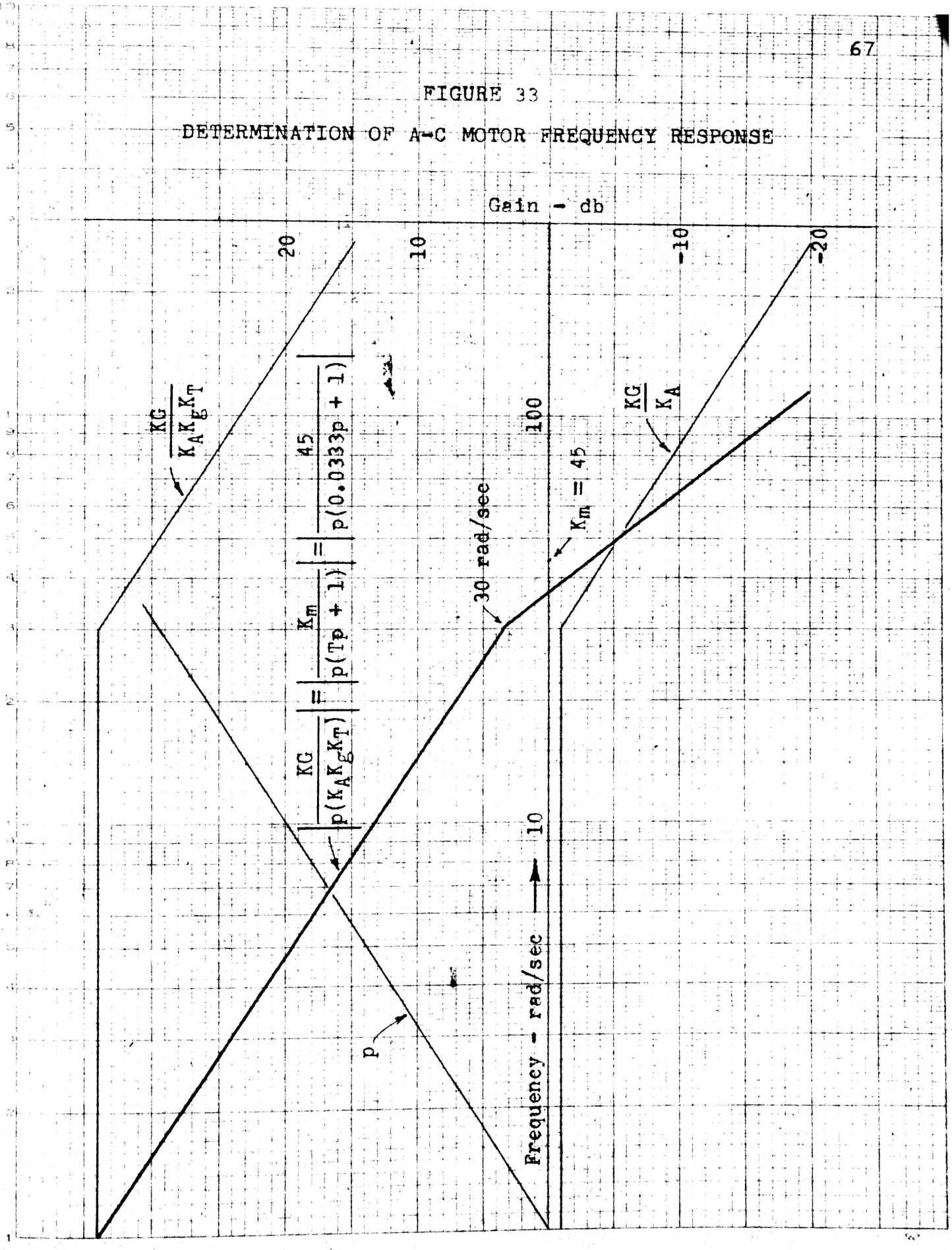

FIGURE 34

COMPARISON OF ANALYTICALLY AND EXPERIMENTALLY OBTAINED A-C SYSTEM FREQUENCY RESPONSE

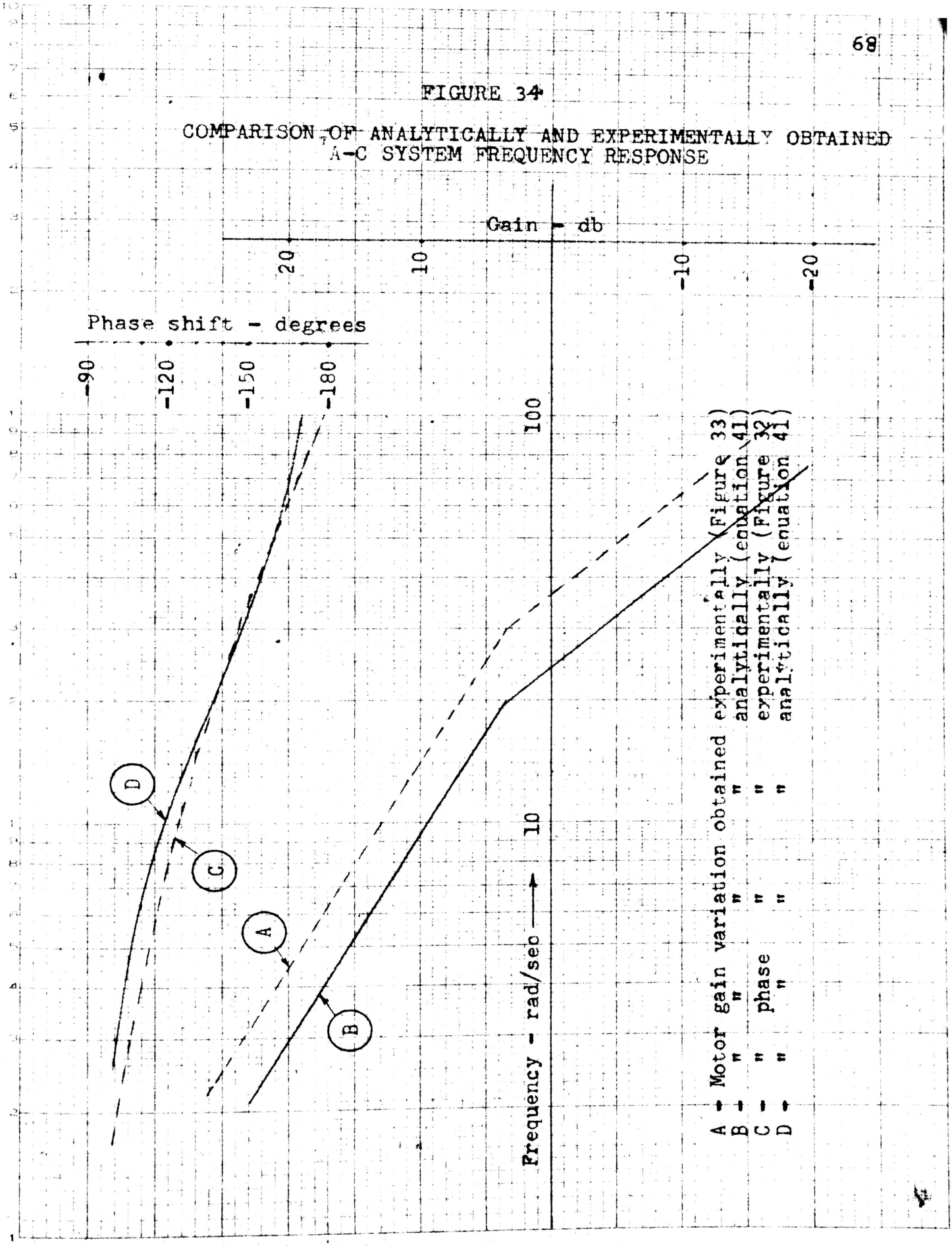

CHAPTER 3

SUMMARY AND CONCLUSION

SUMMARY

By analytical investigation of a d-c motor it was found that the motor transfer function is (equation (17))

$$\frac{0.87}{p(0.0228p + 1)}$$

The motor constants were measured and calculated from the speed-torque characteristics (Figure 6, and 7).

The open loop characteristics of amplidyne and motor where calculated by using the above values and the measured constants of the amplidyne. It was found that the amplidyne-motor transfer function is (equation (35))

$$\frac{36.1}{p(0.078p + 1)(0.077p + 1)}$$

In order to simplify the calculations for frequency response determination, an assumption has been made that a double pole, at 1/0.0775 determine the two time constants of the system.

The transfer function of the 2-phase a-c induction motor was calculated from the speed-torque characteristics given in Figure 11. This transfer function is given in equation (41) as

$$\frac{30}{p(0.0508p + 1)}$$

For graphical determination of frequency response, a simple d-c and a-c systems were designed. Two amplifiers were designed to supply the necessary power, using the system specifications. A function generator was used to supply the input signal, of a sine wave form, to the d-c system. For the a-c system, a suppressed carrier modulated signal was supplied by a pair of synchros.

By considering the proper components transfer function, the amplidyne-motor transfer function was found and given in equation (43)

$$\frac{38}{p(0.0455p + 1)^2}$$

For the a-c system the motor transfer function was found and given in equation (44)

$$\frac{45}{p(0.0333p + 1)}$$

The Equipment Used in Measuring Experimental Data

1) 202A Low Frequency Function Generator

Frequency Range:	.008 to 1200 cps in five decade ranges with wide overlap at each dial extreme.
Dial Accuracy:	Within ±2% from "1.2" to "12" on dial; ±3% from ".8" to "1.2".
Output Waveform:	Sinusoidal, square, and triangular.
Output System:	Can be operated either balanced or single-ended. Output system is direct-coupled.

2) Brush Recorder Mark II

Sensitivity:	10 millivolts per chart line (mm) Fullscale deflection from chart center ±200 millivolts.
Sensitivity steps:	.01, .02, .05, .1, .2, .5, 1, 2, 5, and 10 volts per chart line (mm). Maximum attenuator error 1% with balanced input.
Measurement range	
Single-ended input:	.010 volt to 400 volts.
Balanced input:	.010 volt to 400 volts, side to side, allowable voltage off-ground.
Frequency Response:	The recorded peak-to-peak amplitude of a constant voltage sine wave will be within ±1 chart line (mm) of a nominal 10 lines from d-c to 100 cps.
Trace linearity:	D-c within 1% full chart width. A-c within 2% full chart width, any frequency within limits of maximum amplitude for ink writing.
Chart speed:	1, 5, 25, 125 mm per second.

3) Du Mont Cathode-ray Oscillograph, 304-H

Frequency response	
DC Amplifier:	10% response point at 100 kc.
AC Amplifier	10% response point at 100 kc.
Deflection factor	
Y Attenuator at 1:1,	Y Amplitude Max.=10 rms mv/inch
Y Attenuator at 1:1,	Y Amplitude Min.=115-190 "

CONCLUSION

Experimental study have corroborated the theoretical prediction that it is practical to determine the system frequency response from the components characteristics.

In the d-c system, the different time constants obtained analytically and experimentally, cause the unmatching of the polar plots (Figure 22).

The response of 2-phase induction motor to low frequencies match very nearly that which have been found analytically. At high frequencies, however, the phase shift increased beyond 180 degrees. Such a system can be represented by more than one time constants. A more probable transfer function for the form

$$KG = \frac{K}{p(T_1p + 1)(T_2p + 1)}$$

BIBLIOGRAPHY

1. Truxal, J. G. Control Engineering Handbook. N. Y., McGraw-Hill, 1958

2. Murphy, G. J. Basic Automatic Control. N. Y., Van Nostrand, 1957

3. Savant, C. J. Basic Feedback Control System Design. N. Y., McGraw-Hill, 1958

4. Lawrence, R. R. Principle of Alternating-Current Machinery. N. Y., McGraw-Hill, 1953

5. Gibson, J. E., and Tutteur, F. B. Control System Components. N. Y., McGraw-Hill, 1958

6. Thaler, G. J. Elements of Servomechanism Theory. N. Y., McGraw-Hill, 1955

7. James, H. M., Nichols, N. B., and Philips, R. S. Theory of Servomechanism. N. Y., McGraw-Hill, 1947

8. Steinhacker, M. A., and Messerve, W. E. 2-Phase A-c Servomotor Operation for Varying Phase Angle of the Control Winding Applied Voltage. A.I.E.E. Trans. Vol. 70, pp. 1987-93 (1951)

9. Sobczyk, A. Stabilization of Carrier Frequency Servomechanisms. Franklin Ins. Journal. Vol. 246, pp. 21-44 (July 1948)

10. Koopman, R.J. Operational Characteristic of 2-Phase Servomotor. A.I.E.E. Trans. Vol. 68, part I, pp, 319-329 (1949)

11. Ledgerwood, B. K. Control Engineering Manual. N. Y., McGraw-Hill, 1957

12. Brown, L. O., Jr. Transfer Function for a 2-Phase Induction Servo Motor. A.I.E.E. Trans. Vol. 70 pp. 1890-93 (1951)

13. Thomas, C. H., and Easton, E. C. Graphical Determination of Transfer Function Loci for Servomechanism Components and Systems. A.I.E.E. Trans. Vol. 68, part I, pp. 307-318 (1949)

VITA

The author, son of Mr. and Mrs. Moshe Rachovitsky, was born September 9, 1930 in Tel-Aviv, Israel. He received his elementary education at the Kalia Public School, on the northern shore of the Dead-Sea. His secondary education was obtained at the Public High School in Jerusalem, Israel.

At the end of 1947 he joined the Israel Defense Army. He served during the War of Independence and was discharged as a first Lieutanant in 1951. In September 1952 he started his studies in the Technion - The Israel Institute of Technology and was granted the B.Sc. Degree in Electrical Engineering in 1956. After one year of post graduate training in the Israel Electric Company he came to the United States and enrolled at the Missouri School of Mines and Metallurgy for Graduate studies, in September 1957 having a graduate assistantship.

He married Miss Miriam Rolnizky from Israel, in 1958.